

**DEVELOPMENT OF SUBMERGED ARC WELDING  
FLUXES FOR ENHANCED CORROSION  
RESISTANCE OF STRUCTURAL STEEL WELDS**

**A Thesis**

**Submitted in partial fulfillment of the requirement for the award of degree**

**MASTER OF ENGINEERING  
IN  
PRODUCTION & INDUSTRIAL**

**Submitted By:  
LOCHAN SHARMA  
Roll No. 8009820010**

**Under the Guidance**

**Dr. Rahul Chhibber  
Assistant Professor  
Deptt. of Mechanical Engg.  
Thapar University, Patiala**

**Dr. S.S MALLICK  
Assistant Professor  
Deptt. of Mechanical Engg.  
Thapar University, Patiala**



**DEPARTMENT OF MECHANICAL ENGINEERING  
THAPAR UNIVERSITY  
PATIALA-147004, INDIA**

*Dedicated To My Loving  
Grand Parents*

## CERTIFICATE

This is certify that work done in this thesis report title "DEVELOPMENT OF SUBMERGED ARC WELDING FLUXES FOR ENHANCED CORROSION RESISTANCE OF STRUCTURAL STEEL WELDS" submitted towards partial fulfillment of requirement for award of Master of Engineering degree in Production & Industrial Engineering in Mechanical Engineering Department of Thapar University, Patiala is an authentic record of work carried out by me under the guidance of **Dr. Rahul Chhibber** and **Dr. S.S. Mallick**, Assistant Professor of Mechanical Engineering Department, Thapar University, Patiala.

The matter embodied in this report has not been submitted in part or full to any other university or institute for the award of any degree.

*Lochan Sharma*  
(Lochan Sharma)

This is certifying that above declaration made by the student concerned is correct to the best of my knowledge & belief.

*Rahul Chhibber*  
14/7/2011

**Dr. Rahul Chhibber**

Assistant Professor

Deptt. of Mechanical Engg.

Thapar University, Patiala.

*S.S. Mallick*

**Dr. S.S Mallick**

Assistant Professor

Deptt. of Mechanical Engg.

Thapar University, Patiala

*Ajay Batish*

**Dr. Ajay Batish**

Professor & HOD

Deptt. of Mechanical Engg.

Thapar University, Patiala

Countersigned by:

*S.K. Mohapatra*

**Dr. S.K Mohapatra**

Dean,

Academic Affairs

Thapar University, Patiala

## ACKNOWLEDGEMENT

I am highly grateful to the authorities of Thapar University, Patiala for providing this opportunity to carry out the thesis work.

I express my deep gratitude and respects to my guides **Dr. Rahul Chhibber and Dr. S.S Mallick** for their keen interest and valuable guidance, strong motivation and constant encouragement during the course of the work. I thank them for their great patience, constructive criticism and myriad useful suggestions apart from invaluable guidance to me.

I thank our head of department **Dr. Ajay Batish**, whose excellent leadership made this research project very convenient in term of required staff and nice working condition. I am extremely thankful to member of distinguished faculty.

I would like to thank **Mr. Tajinderpal Singh Sarao** for helping me in various aspects of my research apart from their valuable time.

The non-teaching staff Mr. Surinder Singh, Mr. Surinder Suri, Mr. Sukhbir, Mr. Rajinder Kumar deserve a special thanks for their help during the period of this work.

I am also thankful to other faculty members and all the workshop staff of Mechanical Department, Thapar University, Patiala for their support.

Some friends were never too busy to give me a hand whenever they were needed. No words acknowledge the support I received from **Karanpreet Singh, Sumit, Manjot, Rajdeep, Sorav, Aseem** for their valorous help and co-operation.

Last but not the least, I would like to thank my **grandfather, parents, uncle, sister, brothers** for always being there when I needed them most and for their moral support that kept my spirit up during the endeavor.

*Lochan Sharma*  
LOCHAN SHARMA

## **ABSTRACT**

The present study aims at investigating the effect of submerged arc welding fluxes for enhanced corrosion resistance of structural steel welds. Corrosion resistance and mechanical properties of weld metal such as tensile strength, impact strength, micro-hardness and micro-structure in submerged arc weldments are evaluated. A combined approach of experimental and analytical methods is used and models for corrosion resistance and mechanical properties in terms of welding parameters is developed.

## **TABLE OF CONTENTS**

<b>S. No.</b>	<b>Topic</b>	<b>Page No.</b>
	<b>Certificate</b>	III
	<b>Acknowledgement</b>	IV
	<b>Abstract</b>	V
	<b>List of Tables</b>	IX
	<b>List of Figures</b>	X-XII
	<b>Chapter 1</b>	
	<b>INTRODUCTION</b>	
1.1	Welding	1
1.2	Submerged arc welding	1
1.3	Submerged arc welding equipment	2
1.4	Submerged arc Process variables	2
1.5	Effect of Welding Parameters on Welding	3
1.5.1	Welding Current	3
1.5.2	Arc Voltage	3
1.5.3	Welding Speed	3
1.6	Advantages of SAW	4
1.7	Limitations of SAW	4
1.8	Application	4
1.9	Welding Flux	5
1.9.1	Types of fluxes	5
1.9.2	Fused fluxes	5
1.9.3	Agglomerated fluxes	6
1.10	Plain carbon alloy steel	6
1.10.1	Types	6
(a)	Mild and Low carbon steel	6
(b)	High carbon steel	7
(c)	Medium carbon steel	7
1.10.2	Applications	9
1.11	Corrosion	9
1.12	Types of Corrosion	10
(A)	Uniform Corrosion	11
(B)	Localized Corrosion	11
(C)	Galvanic Corrosion	13

(D)	Crevice Corrosion	14
(E)	Stress Corrosion Cracking	15
(F)	Pitting Corrosion	16
(G)	Selective Attack	16
(H)	Stray Current Corrosion	17
(I)	Microbial Corrosion	18
(J)	Intergranular Corrosion	18
(K)	Thermo galvanic Corrosion	18
1.13	Corrosion Testing	19
	Electrochemical Measurement	19
	Potential Measurement	19
	Potentiodynamic Measurement	20
1.14	Electrochemical Measurement	20
1.15	Potential Measurement	20
	<b>Chapter 2</b>	
	<b>LITERATURE REVIEW</b>	21-34
	<b>Chapter 3</b>	
	<b>PROBLEM FORMULATION</b>	35
	<b>Chapter 4</b>	
	<b>EXPERIMENTATION</b>	
4.1	Method of preparation flux	38
4.2	Basicity Index	41
4.3	Chemical composition of Base metal	43
4.4	Chemical composition of electrode	43
4.5	Method of preparation of steel specimen	52
4.6	Corrosion Test	53
4.7	Tensile Test	55
4.8	Impact Test	56
4.9	Microstructure	57
4.10	Micro hardness	58
4.11	Chemical Composition	59
4.12	SEM	60
	<b>Chapter 5</b>	
	<b>RESULTS AND DISCUSSIONS</b>	
5.1	Impact Toughness Test	62
5.2	Corrosion Test	66
5.3	Microstructure	70

5.4	Micro hardness Test	74
5.5	Tensile Test	80
5.6	Chemical composition of weld metal	87
5.7	Scanning Electron Microscope (SEM)	91
	<b>Chapter 6</b>	
	<b>CONCLUSION &amp; FUTURE SCOPE</b>	
6.1	Conclusion	92
6.2	Scope of future work	93
	<b>REFERENCES</b>	95

## LIST OF TABLE

<b>Table Number</b>	<b>Description</b>	<b>Page No.</b>
4.1	Test Matrix	36
4.2	Chemical composition of Flux 1	37
4.3	Chemical Composition of Flux 2	37
4.4	Chemical Composition of Flux 3	38
4.5	Chemical Composition of Flux 4	38
4.6	Chemical Composition of Flux 5	39
4.7	Chemical Composition of Flux 6	39
4.8	Chemical Composition of Flux 7	39
4.9	Basicity Index	39
4.10	Chemical Composition of base metal	40
4.11	Chemical Composition of electrode	40
5.1	Impact Test	51
5.2	Corrosion Rate by Polarization Scan	53
5.3	Standard values of Half Cell Potential	57
5.4	Corrosion Testing of Specimen	57
5.5	Weight loss	59
5.6	Micro hardness values at welded region	64
5.7	Ultimate tensile strength	68
5.8	Ultimate tensile stress	69
5.9	Percentage Change and Change in Percentage Composition of Carbon and Manganese	71
5.10	Percentage Change and Change in Percentage Composition of Silicon and Chromium	72

## **LIST OF FIGURES**

<b>Figure Number</b>	<b>Description</b>	<b>Page No.</b>
1.1	Submerged arc welding machine	1
1.2	Flux	5
1.3	Carbon steel pressure vessel	7
1.4	Mild steel pressure vessel	8
1.5	Aluminum pressure vessel	8
1.6	Uniform corrosion	10
1.7	Localized corrosion	11
1.8	Galvanic corrosion	12
1.9	Crevice corrosion	13
1.10	Stress corrosion cracking	14
1.11	Pitting corrosion	15
1.12	Selective corrosion attack	16
1.13	Stray current corrosion	16
1.14	Microbial corrosion	16
1.15	Intergranular corrosion	17
1.16	Thermo galvanic corrosion	18
4.2	Compounds mix with Binder	40
4.3	Flux after mixing	40
4.4	Test sieve	40
4.5	Tacking on back side of plates	41
4.6	Submerged Arc Welding of plates(a,b,c)	42
4.7	Cutting of plates after welding	43
4.8	Cutting of plates on surface grinder	44
4.9	Cutting of Plates according to required size	44
4.10	Plates after grinding from weld area	44
4.11	Specimens before Corrosion Test	45
4.12	Saturated calomel electrode (SCE)	45
4.13	Orientation of a typical tensile test specimen	46
4.14	Specimens used for Tensile Testing	46
4.15	Standard Charpy test specimen	47
4.16	Specimens used for Impact Testing	47
4.17	Pieces for Microstructure & Micro hardness	48
5.1	Specimens after charpy test	50

5.2	Impact Toughness	50
5.3	Specimens after Corrosion Test by Polarization Scan	51
5.4	Corrosion potential ( $E_{\text{corr}}$ ) and Corrosion current ( $I_{\text{corr}}$ ) for base metal	52
5.5	Corrosion potential ( $E_{\text{corr}}$ ) and Corrosion current ( $I_{\text{corr}}$ ) for Flux 1	53
5.6	Corrosion potential ( $E_{\text{corr}}$ ) and Corrosion current ( $I_{\text{corr}}$ ) for Flux 2	53
5.7	Corrosion potential ( $E_{\text{corr}}$ ) and Corrosion current ( $I_{\text{corr}}$ ) for Flux 3	54
5.8	Corrosion potential ( $E_{\text{corr}}$ ) and Corrosion current ( $I_{\text{corr}}$ ) for Flux 4	54
5.9	Corrosion potential ( $E_{\text{corr}}$ ) and Corrosion current ( $I_{\text{corr}}$ ) for Flux 5	55
5.10	Corrosion potential ( $E_{\text{corr}}$ ) and Corrosion current ( $I_{\text{corr}}$ ) for Flux 6	55
5.11	Corrosion potential ( $E_{\text{corr}}$ ) and Corrosion current ( $I_{\text{corr}}$ ) for Flux 7	56
5.1 2	Corrosion test by Half-Cell Potential	58
5.13	Specimens in water bowl	58
5.14	Specimens in water bowl and samples in water with scale	58
5.15	%age change in weight	59
5.16	Microstructure of flux 1 at x500 magnification	60
5.17	Microstructure of flux 2 at x500 magnification	60
5.18	Microstructure of flux 3 at x500 magnification	61
5.19	Microstructure of flux 4 at x500 magnification	62
5.20	Microstructure of flux 5 at x500 magnification	62
5.21	Microstructure of flux 6 at x500 magnification	63
5.22	Microstructure of flux 7 at x500 magnification	63
5.23	Micro hardness of Base metal	65
5.24	Micro hardness of flux 1	65
5.25	Micro hardness of flux 2	65
5.26	Micro hardness of flux 3	65
5.27	Micro hardness of flux 4	65
5.28	Micro hardness of flux 5	65
5.29	Micro hardness of flux 6	66
5.30	Micro hardness of flux 7	66
5.31	Micro hardness with different fluxes	66
5.32	Specimen after tensile test	67
5.33	Load vs. Disp. Curve for base metal	67
5.34	Stress vs. Strain Curve for base metal	68
5.35	Load vs. Disp. Curve for 7 different fluxes	69
5.36	Stress vs. Strain Curve 7 different fluxes	70
5.37	Specimens after checking composition	71
5.38	Percentage Composition of C, Mn, Si and Cr in weld metal	72

5.39	Percentage Change in Composition of C, Mn, Si and Cr in weld metal	73
5.40	SEM measurement at x1000 magnification for specimen after breakage of tensile test which weld from by using welding flux (1), (2), (3), (4), (5), (6), (7)	75
5.41	SEM measurement at x1000 magnification for specimen after breakage of tensile test which weld from by using welding flux (1), (2), (3), (4), (5), (6), (7)	76

**1.1 WELDING**

Welding as it is normally understood today is comparatively a new comer amongst the fabrication processes though smith forging to join metal pieces was practiced even before Christ. Though there are a number of well established welding processes but arc welding with coated electrodes is still the most popular welding process the world over. Arc welding in its present form appeared on the industrial scene in 1880's. Arc welding, however, was not accepted for fabrication of critical components till about 1920 by which time coatings for electrodes had been well developed. <sup>[1]</sup>

**1.2 SUBMERGED ARC WELDING**

Submerged Arc Welding is a fusion welding process in which heat is produced from an arc between the work and a continuously fed filler metal electrode. The molten weld pool is protected from the surrounding atmosphere by thick blanket of molten flux and slag formed from the granular fluxing material pre-placed on the work. <sup>[1]</sup>



**Fig. 1.1: Submerged Arc Welding Machine**

### **1.3 SUBMERGED ARC WELDING EQUIPMENT**

Equipment for submerged arc welding depends upon whether the process is of the automatic type or the semi-automatic type. For automatic submerged arc welding it consists of a welding power source, a wire feeder and a control system, an automatic welding head, a flux hopper with flux feeding mechanism, a flux recovery system and a travel mechanism which usually consists of a travelling carriage and the rails. A power source for automatic submerged arc welding process must be rated for 100% duty cycle as the weld often takes more than 10 times to complete.

Both AC and DC power sources are used and they may be of constant current (CC) or constant voltage (CV) type. Submerged arc welding is a high current welding process; the equipment is designed to produce high deposition rates. For single arc, DC power source with CV is almost invariably employed while AC power sources are most often used for multi-electrode submerged arc welding. Generally, welding rectifiers are employed as power sources for getting a current range of 50A to 2000A, however most often submerged arc welding is done with a current range of 200 to 1200A.

The welding gun for automatic submerged arc welding is attached to the wire feed motor and include current pick up tips for providing the electrical contact to the wire electrode. The flux hopper is attached to the welding head and it may be magnetically operated through valves so that they can be opened or closed by control system. <sup>[1]</sup>

### **1.4 SUBMERGED ARC WELDING PROCESS VARIABLES**

The important process variables in submerged arc welding include the welding current, arc voltage and welding speed. However, the weld bead geometry is also affected considerably by electrode-to-work angle, inclination of the work piece (uphill or downhill), joint edge preparation, electrode stick out, the kind of current and polarity, electrode diameter, and the type and grain size of the flux. The affect of these process variables are determine through effects on weld bead geometry. Due to high heat input in SAW the weld pool, i.e., the layer of molten metal between the arc and the parent un melted metal is of considerable extent and as this layer is of low thermal conductivity it has , therefore, a marked effect on the depth of

penetration. Thus, an increase in depth of this molten metal layer is accompanied by an increase in depth of penetration. <sup>[1]</sup>

## **1.5 WELDING PARAMETERS AND THEIR EFFECTS**

### **1.5.1 Welding Current:**

The increase in welding current the pressure exerted by the arc increases which drives out the molten metal from beneath the arc and that lead to increased depth of penetration. The width of weld remains almost unaffected. As increased welding current is accompanied by increase in wire feed rate, it results in greater weld reinforcement. Variation in current density has nearly the same effect on weld geometry as the variation in magnitude of current. Welding with DCNP produces deeper penetration than DCNP. For a given welding current, a decrease of wire diameter results in increase in current density. This results in a weld with deeper penetration but of somewhat reduced width. The submerged arc welding process usually employs wires of 2 to 5mm diameter, thus for deeper penetration at low currents a wire of diameter 2 to 3mm is best suited.

### **1.5.2 Arc Voltage:**

Arc voltage varies in direct proportion to the arc length. With the increase in arc length the arc voltage increases and thus more heat is available to melt the metal and the flux. However, increased arc length means more spread of arc column, this leads to increase in weld width and volume of reinforcement while the depth of penetration decreases. The arc voltage varies with welding current and wire diameter, and in SAW it usually ranges between 30 to 50 volts.

### **1.5.3 Welding Speed:**

With increase in welding speed, the width of weld decreases. However, if the increase in speed is small the depth of penetration increases because the layer of molten metal is reduced which leads to higher heat conduction towards the bottom of the plate. With further increase in welding speed, above 40 m/hour, the heat input per unit length of the weld decreases considerably and the depth of penetration is thus reduced. At speed above 80 m/hour, lack of fusion may result. It has been established experimentally that as a first approximation the welding speed,  $S$ , for a well shaped weld should be based on the following relationship. <sup>[1]</sup>

$$S = 2500/I_n \text{ m/hour}$$

Where  $I_n$  is the welding current in amperes.

## **1.6 THE ADVANTAGES OF SAW**

The following are the advantages of SAW:

- ✓ High deposition rates (45 kg/h) have been reported.
- ✓ High operating factors in mechanized applications.
- ✓ Deep weld penetration.
- ✓ Sound weld are readily made (with good process design and control)
- ✓ High speed welding of thin sheet steels up to 5 m/mm (16 ft/min) is possible.
- ✓ Minimal welding fume or arc light is emitted.
- ✓ Practically no edge preparation is necessary.
- ✓ The process is suitable both indoor and outdoor works.
- ✓ Distortion is much less.
- ✓ Welds produced are sound, uniform, ductile, and corrosion resistant and have good impact value.
- ✓ 50 to 90 % of flux is recoverable. <sup>[2]</sup>

## **1.7 LIMITATIONS OF SAW**

The following are the limitations of SAW:

- ✓ Limited to ferrous (steel or stainless steels) and some nickel based alloys.
- ✓ Normally limited to long straight seams or rotated pipes or vessels.
- ✓ Requires relatively troublesome flux handling systems.
- ✓ Flux and slag residue can present a health & safety concern.
- ✓ Requires inter-pass and post weld slag removal. <sup>[2]</sup>

## **1.8 APPLICATIONS OF SAW**

The following are the applications of SAW:

- ✓ SAW is used for welding low carbon and medium carbon steel.
- ✓ For welding stainless steels, copper, aluminum, and titanium base alloys.
- ✓ SAW is also capable of welding heat resistant steels, corrosion resistant steels and high strength steels.

- ✓ SAW is widely used for butt and fillet welds in heavy industries like shipbuilding, pressure vessel fabrication, rail-road tank cars, structural engineering, pipe welding, and for storage tanks.
- ✓ Thinner material products such as water heaters and propane tanks
- ✓ Hard facing for steel mills, earthmoving equipment, mining, etc. <sup>[1]</sup>

## **1.9 SUBMERGED ARC WELDING FLUX**

The flux protects the molten pool and the arc against atmospheric oxygen and nitrogen by creating an envelope of molten slag. The slag also cleanses the weld metal (i.e. deoxidizes it and removes impurities such as sulphur) modifies its chemical composition and controls the profile of the weld bead. The molten slag also provides favorable conditions for very high current densities, which together with the insulating properties of the flux; concentrate intense heat into a relatively small welding zone. <sup>[1]</sup>



**Fig. 1.2: Flux**

### **1.9.1 Types of Fluxes**

Two main types of submerged arc fluxes are available, depending on the method of manufacture i.e. fused and agglomerated.

### **1.9.1.1 Fused Flux**

Fused fluxes are more tolerant to mill scale, oil, grease and dirt on work surface. Fused fluxes may also pick up moisture when stored under humid atmosphere, but they can tolerate a large percentage of moisture in terms of weld metal porosity. They require less drastic heating to remove the picked up moisture. Fused flux are non-hygroscopic, fully reacted, chemically homogeneous, contain no metallic deoxidizers, glass-like appearance and high grain strength. Fused fluxes provide smooth, stable performance at high welding currents.

### **1.9.1.2 Agglomerated Flux**

Agglomerated fluxes produce weld deposits of better ductility and impact strength as compared with fused fluxes. Alloy transfer efficiency is also better in case of agglomerated fluxes and, therefore they are preferred when high percentage of alloy transfer from the flux is required. Agglomerated fluxes have lower bulk density and hence under identical welding parameters less flux is melted for a given amount of weld deposit as compared with fused fluxes. However, agglomerated fluxes react to moisture in the same way as low hydrogen electrode, i.e., they tend to give weld metal porosity at even low moisture level. Hence, they require more thorough drawing before use as compared to fused fluxes. Agglomerated flux contains metallic deoxidizers, contain alloying agents, flat, low gloss, or dry particle appearance. <sup>[1]</sup>

Agglomerated flux provides good performance over rust and mill scale and helps prevent weld porosity. It provides better peeling properties than fused fluxes. Alloying elements can be added to provide improved chemical and mechanical properties.

## **1.10 PLAIN CARBON STEEL**

Carbon steel also called plain-carbon steel where the main interstitial alloying constituent is carbon. The American Iron and Steel Institute(AISI) defines carbon steel as Steel is considered to be carbon steel when no minimum content is specified or required for chromium, cobalt, niobium, molybdenum, nickel, titanium, tungsten, vanadium or zirconium or any other element to be added to obtain desired alloying effect, when the specified minimum for copper does not exceed 0.40% .<sup>[2]</sup>

### **1.10.1 Types of Plain Carbon Steel**

#### **(a) Mild and low carbon steel**

Mild steel is the most common form of steel because its price is relatively low while it provides material properties that are acceptable for many applications. Low carbon steel contains approximately 0.05–0.15% carbon and mild steel contains 0.16–0.29% carbon, therefore it is neither brittle nor ductile. Mild steel has a relatively low tensile strength, but it is cheap and malleable; surface hardness can be increased through carburizing.

It is often used when large quantities of steel are needed, for example as structural steel. It is often used when large quantities of steel are needed, for example as structural steel. The density of mild steel is approximately  $7.85 \text{ g/cm}^3$  ( $0.284 \text{ lb/in}^3$ ) and the Young's modulus is  $210,000 \text{ Mpa}$  ( $30,000,000 \text{ psi}$ ).<sup>[2]</sup>

#### **(b) High carbon steel**

Carbon steels which can successfully undergo heat-treatment have carbon content in the range of 0.30–1.70% by weight. Trace impurities of various other elements can have a significant effect on the quality of the resulting steel. Trace amounts of sulfur in particular make the steel red-short. Low alloy carbon steel, such as A36 grade, contains about 0.05% sulfur and melts around  $1426\text{--}1538 \text{ }^\circ\text{C}$  ( $2599\text{--}2800 \text{ }^\circ\text{F}$ ).<sup>[2]</sup>

#### **(c) Medium carbon steel**

Approximately 0.30–0.59% carbon content. Balances ductility and strength and has good wear resistance; used for large parts, forging and automotive components.<sup>[2]</sup>

### **1.10.2 Application of Carbon Steel**

Low Carbon Steel Pressure Vessels is widely known for its unbeatable performance. These have a large capacity to hold gases and liquids at high temperatures. Latest international technology is employed for manufacturing these vessels. Hence, Carbon Steel Pressure Vessels find extensive usage for various industrial purposes.



**Fig. 1.3 : Carbon Steel Pressure Vessel** <sup>[3]</sup>

Mild Steel Pressure Vessels are also known for its unbeatable performance. Premium quality mild steel is used in making of these vessels. Further, these vessels are designed and used for storing liquids and gases at a constant temperature and pressure, which varies from the surrounding pressures. Hence, these are aptly used for various purposes in industrial and private sector.



**Fig. 1.4: Mild Steel Pressure Vessel** <sup>[3]</sup>

Aluminum Pressure Vessels are also widely used in the market. These are specially designed in a closed shape to hold liquids and gases at a pressure, different from outside pressure. This product is leak proof, corrosion resistant, and durable.



**Fig. 1.5: Aluminum Pressure Vessel** <sup>[3]</sup>

Since Latest international technology is employed for manufacturing these vessels e.g. Submerged Arc Welding now days. Submerged arc welding is a fusion arc welding process in which heat is produced from an arc between the work and continuously fed filler metal electrode. The molten weld pool is protected from the surrounding atmosphere by thick blanket of molten flux and slag formed from the granular fluxing material pre-placed on the work. There are various advantages of SAW such as higher deposition rate, efficient use of material, minimum operator protection required, semi-skilled operator can be employed, high quality weld produced, weld size up to 25mm in one pass can be made etc. Hence due to these benefits SAW is extensively used in various pressure vessels construction. For smooth operation of process better quality control of product and to satisfy safety norms it should required that pressure vessels do not fail, i.e. pressure vessels joint do not lose their strength due to their prolonged exposure to chemicals and/or high temperature and/or pressure of the process conditions. One important factor that has been reported to cause damage to the weld joints is corrosion.

### **1.11 CORROSION**

When water contains less iron than the maximum that it is capable of carrying in solution, it corrodes iron or steel rapidly unless a protective film or crust of some material covers the metal surface. The unsaturated water tends to dissolve metal from the surface of well screens, well casing or piping systems until it becomes saturated with respect to iron, if the

mineral content of the water is such that a protective film is not formed by deposition of insoluble materials, severe corrosion results. <sup>[4]</sup>

The following are the factors affecting corrosion:

- fluid (or metal temperature)
- fluid flow rate
- metal or combination of metals
- metal working (forming or welding)
- maintenance or cleaning frequency
- fouling
- film formation

## **1.12 TYPES OF CORROSION**

Following are the types of corrosion:

### **A) Uniform Corrosion**

Uniform corrosion, as the name suggests, occurs over the majority of the surface of a metal at a steady and often predictable rate. Although it is unsightly its predictability facilitates easy control, the most basic method being to make the material thick enough to function for the lifetime of the component. <sup>[5]</sup>

Uniform corrosion can be slowed down or stopped by using the five basic facts:

- (1) Slow down or stop the movement of electrons.
  - (a) Coat the surface with a non-conducting medium such as paint, lacquer or oil
  - (b) Reduce the conductivity of the solution in contact with the metal an extreme case being to keep it dry. Wash away conductive pollutants regularly.
  - (c) Apply a current to the material (see cathode protection).
- (2) Slow down or stop oxygen from reaching the surface. Difficult to do completely but coatings can help.
- (3) Prevent the metal from giving up electrons by using a more corrosion resistant metal higher in the electrochemical series. Use a sacrificial coating which gives up its electrons more easily than the metal being protected. Apply cathode protection. Use inhibitors.
- (4) Select a metal that forms an oxide that is protective and stops the reaction.



**Fig. 1.6: Generalized Corrosion or Uniform Corrosion** <sup>[4]</sup>

### **B) Localized Corrosion**

The consequences of localized corrosion can be a great deal more severe than uniform corrosion generally because the failure occurs without warning and after a surprisingly short period of use or exposure.<sup>[5]</sup>



**Fig. 1.7: Localized Corrosion** <sup>[4]</sup>

### **C) Galvanic Corrosion**

Galvanic corrosion, Bimetallic Corrosion or Dissimilar Metal Corrosion, as sometimes called, is defined as the accelerated corrosion of a metal because of an electrical contact (including physical contact) with a more noble metal or nonmetallic conductor (the cathode) in a corrosive electrolyte. The less corrosion resistant or the "active" member (anodic) of the couple experiences accelerated corrosion while the more corrosion resistant or the "noble" member of the couple experiences reduced corrosion due to the "cathode protection" effect. The most severe attack occurs at the joint between the two dissimilar metals. Further away from the bi-metallic joint, the degree of accelerated attack is reduced.

For an example of galvanic corrosion, consider a system is composed of 316 SS (a very noble alloy - meaning it is quite resistant to corrosion and has a low galvanic potential) and a mild steel (a very active metal with high galvanic potential). The mild steel will corrode in the presence of an electrolyte such as salt water. If a sacrificial anode is used (such as a zinc alloy, aluminum alloy, or magnesium), these anodes will corrode, protecting the other metals.<sup>[5]</sup>

### **Mechanism**

When two or more different sort of metals come into contact in the presence of an electrolyte a galvanic couple is set up as different metals have different electrode potentials. The electrolyte provides a means for ion migration whereby metallic ions can move from the anode to the cathode. This leads to the anodic metal corroding more quickly than it otherwise would; the corrosion of the cathode metal is retarded even to the point of stopping. The presence of electrolyte and a conducting path between the metals may cause corrosion where otherwise neither metal alone would have corroded.

The potential difference (i.e., the voltage) between two dissimilar metals is the driving force for the destructive attack on the active metal (anode). Current flows through the electrolyte to the more noble metal (cathode) and the less noble (anode) metal will corrode. The conductivity of electrolyte will also affect the degree of attack. The cathode to anode area ratio is directly proportional to the acceleration factor.<sup>[5]</sup>



**Fig. 1.8: Galvanic Corrosion** <sup>[4]</sup>

## **Prevention and Control**

- Galvanic corrosion can be prevented through a number of methods
- Select metals/alloys as close together as possible in the galvanic series
- Avoid unfavorable area effect of a small anode and large cathode
- Insulate dissimilar metals wherever practical
- Apply coatings with caution. Paint the cathode (or both) and keep the coatings in good repair on the anode.
- Avoid threaded joints for materials far apart in the galvanic series
- When galvanic potential exists, design with appropriate thickness in the anodic metal when practical.

## **D) Crevice Corrosion**

Crevice Corrosion refers to the localized attack on a metal surface at, or immediately adjacent to, the gap or crevice between two joined surfaces. The gap or crevice can be formed between two metals or a metal and non-metallic material. Outside the gap or without the gap, both metals are resistant to corrosion.

The damage is normally confined to one metal at localized area within or close to the joining surfaces. Common locations for Crevice Corrosion in heat exchangers are at a gap between the tube and tube sheet or at gasket joints. <sup>[5]</sup>

### **Mechanism**

Crevice corrosion generally occurs due to either high concentration of impurities in the crevice (e.g., chlorides, acid, or base), or differential electrolyte chemistry inside and outside the crevice: a single metal part undergoing corrosion is submerged in two different environments.

Crevice corrosion is initiated by a difference in concentration of some chemical constituents, usually oxygen, which set up an electrochemical concentration cell (differential aeration cell in the case of oxygen). <sup>[5]</sup>



**Fig. 1.9: Crevice Corrosion** <sup>[4]</sup>

### **Prevention**

- Use welded butt joints instead of riveted or bolted joints in new equipment
- Eliminate crevices in existing lap joints by continuous welding or soldering
- Use solid, non-absorbent gaskets such as Teflon.
- Use higher alloys for increased resistance to crevice corrosion

### **E) Stress Corrosion Cracking**

Stress-corrosion cracking (SCC) is a cracking process that requires the simultaneous action of corroded and sustained tensile stress. This excludes corrosion-reduced sections that fail by fast fracture. It also excludes intercrystalline or transcrystalline corrosion, which can disintegrate an alloy without applied or residual stress. Stress-corrosion cracking may occur in combination with hydrogen embrittlement.

### **Mechanism**

Stress corrosion cracking results from the conjoint action of three components:

- (1) A susceptible material
- (2) A specific chemical species (environment)
- (3) Tensile stress

For example, copper and its alloys are susceptible to ammonia compounds, mild steels are susceptible to alkalis and stainless steels are susceptible to chlorides.

Stress corrosion cracking presents an especially difficult problem, since not only is it highly localized but it can occur in environments that are merely mildly corrosive to the material. The damaging concentration of the harmful ions in that environment may be quite

small and difficult to detect and, even in the absence of applied stress, residual stresses in a structure can often be of a sufficiently high level to cause SCC and failure in service.<sup>[5]</sup>

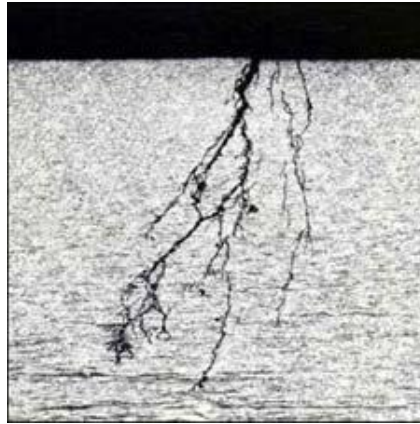


**Fig. 1.10: Stress Corrosion Cracking**<sup>[4]</sup>

### **Prevention**

- Control of stress level (residual or load) and hardness.
  - Avoid the chemical species that causes SCC.
  - Use of materials known not to crack in the specified environment.
  - Control temperature and or potential

### **F) Pitting Corrosion**

Pitting corrosion occurs in materials that have a protective film such as a corrosion product or when a coating breaks down. The exposed metal gives up electrons easily and the reaction initiates tiny pits with localized chemistry supporting rapid attack.<sup>[5]</sup>

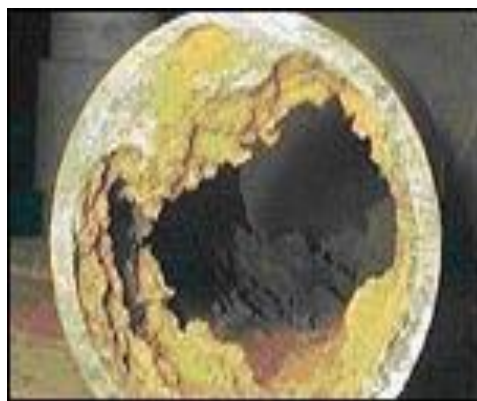


**Fig. 1.11: Pitting Corrosion**<sup>[4]</sup>

### **Control can be ensured by:**

- Selecting a resistant material
- Ensuring a high enough flow velocity of fluids in contact with the material or
- frequent washing
- Control of the chemistry of fluids and use of inhibitors
- Use of a protective coating
- Maintaining the material's own protective film.<sup>[5]</sup>

### **G) Selective Attack**

This occurs in alloys such as brass when one component or phase is more susceptible to attack than another and corrodes preferentially leaving a porous material that crumbles. It is best avoided by selection of a resistant material but other means can be effective such as:

- Coating the material
- Reducing the aggressiveness of the environment
- Use of cathode protection

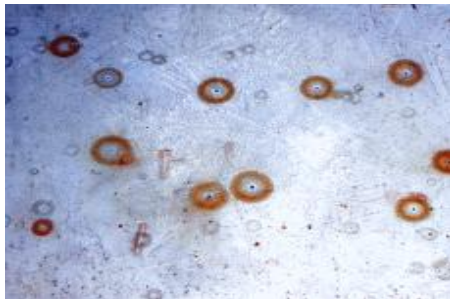


**Fig. 1.12: Selective Corrosion Attack** <sup>[4]</sup>

### **H) Stray Current Corrosion**

When a direct current flows through an unintended path and the flow of electrons supports corrosion. This can occur in soils and flowing or stationary fluids.

The most effective remedies involve controlling the current by:

Insulating the structure to be protected or the source of current

- Earthling sources and/or the structure to be protected.
- Applying cathode protection
- Using sacrificial targets.



**Fig.1.13: Stray Current Corrosion** <sup>[4]</sup>

### **I) Microbial Corrosion**

This general class covers the degradation of materials by bacteria, moulds and fungi or their by-products. It can occur by a range of actions such as:

- Attack of the metal or protective coating by acid by-products, sulphur, hydrogen sulfide or ammonia
- Direct interaction between the microbes and metal which sustains attack.<sup>[5]</sup>



**Fig .1.14: Microbial Corrosion** <sup>[4]</sup>

**Prevention can be achieved by:**

- Selection of resistant materials
- Frequent cleaning
- Control of chemistry of surrounding media and removal of nutrients
- Use of biocides
- Cathode protection

## J) Inter granular Corrosion

This is preferential attack of the grain boundaries of the crystals that form the metal. It is caused by the physical and chemical differences between the centers and edges of the grain.

It can be avoided by:

- Selection of stabilized materials
- Control of heat treatments and processing to avoid susceptible temperature range.



**Fig.1.15: Intergranular Corrosion** <sup>[4]</sup>

## K) Thermo galvanic Corrosion

Temperature changes can alter the corrosion rate of a material and a good rule of thumb is that  $10^0$  C rise doubles the corrosion rate. If one part of component is hotter than another the difference in the corrosion rate is accentuated by the thermal gradient and local attack occurs in a zone between the maximum and minimum temperatures. The best method of prevention is to design out the thermal gradient or supply a coolant to even out the difference. <sup>[5]</sup>



**Fig. 1.16: Thermo galvanic Corrosion** <sup>[4]</sup>

### **1.13 CORROSION TESTING**

Electrochemical techniques are the most widely used techniques for the study of corrosion in laboratories together with their application to real life structures and various pressure vessels such as boilers, steam turbines, heat exchangers etc. The reason for the frequent use of electrochemical techniques in practice is the increased demand of pressure vessels which require an assessment of their residual health condition due to the premature deterioration caused by reinforcement corrosion. In addition it is necessary to evaluate the short-term performance of different components to know their early age behavior by performing various corrosion tests at initial periods. <sup>[2]</sup>

The commonly used techniques are:

1. Electrochemical measurement,
2. Potential measurement,
3. Potentiodynamic polarization measurement,
4. Electrochemical impedance measurement etc

### **1.14 ELECTROCHEMICAL MEASUREMENT**

The corrosion medium is 0.9wt% NaCl neutral solution, prepared by analytical sodium chloride and distilled water. The test system is a 3-electrode system, the sample is the working electrode, and the reference electrode is a saturated calomel electrode and a platinum plate serves as the counter electrode. In this experiment the features of the electrochemical noise and polarization curves are studied. The electrochemical measurements were performed using a potentiostat/frequency response analyzer (ACM instruments, UK).

The sampling rate of the EN tests is 10 Hz and the potential noise is recorded. The potential noise recorded in this experiment is the fluctuation of the electrode potential between the working electrode and the reference electrode. Besides the EN measurements, the corrosion behaviour of the two materials are also studied by potentiodynamic polarization curves, the scan rate of the potentiodynamic tests is 1 mV/s. All the experiments are carried out at room temperature. <sup>[2]</sup>

## **1.15 POTENTIAL MEASUREMENT**

The detection of corrosion by using the method of potential measurement is one of the most common procedures for the routine inspection of metals or alloys. The half-cell potential is measure of electrode potential, represents the potential difference between the metal and the adjacent electrolyte. Thus in a given environment it may serve as an indicator of corrosion initiation since the threshold of depassivation depends mainly on the potential compared.

The half-cell potential value is measured with reference to a standard reference electrode. The various reference electrodes used for the potential measurement are standard hydrogen electrode (SHE), copper-copper sulphate electrode (Cu/CuSO<sub>4</sub>), saturated calomel electrode (SCE), silver-silver chloride electrode (Ag/AgCl), and mercury-mercurial sulphate electrode (Hg/HgSO<sub>4</sub>).

The factors affecting potential measurements are reference electrode position, polarization phenomena induced by limited oxygen diffusion, presence of cracks, stray currents. Nonetheless, this technique is widely used as a first approach for corrosion detection. However quantification and reliable prediction of the corrosion rate requires the use of other electrochemical techniques. <sup>[2]</sup>

## **1.16 AC IMPEDANCE SPECTROSCOPY TECHNIQUE**

AC impedance spectroscopy also sometimes known as the electrochemical impedance spectroscopy (EIS) is a technique working in frequency domain. The concept involved in this technique is that an electrochemical interface can be viewed as a combination of passive electrical circuit elements namely resistance and capacitance.

The AC impedance technique involves the application of a small-amplitude sinusoidal potential to the working electrode at a number of discrete frequencies. At each one of these frequencies, the resulting current waveform will exhibit a sinusoidal response that is out of phase with the applied potential signal by a certain amount and has current amplitude that is inversely proportional to the impedance of the interface. Due to sophistication of the measurement, AC impedance spectroscopy technique is more frequently used in laboratory studies rather than in field surveys. Further often it is difficult to interpret and is a time-consuming technique. Nevertheless, its use is nowadays a powerful tool to understand the

behaviour of the matrix/composite interface and provides information about the mechanism of corrosion reaction at the matrix/composite interface and the corrosion kinetics etc. <sup>[2]</sup>

[1] **Serdar Karaoglua et al. [2008]** observed process parameters that have great influence on the quality of a welded connection. Mathematical modeling can be utilized in the optimization and control procedure of parameters. Rather than the well-known effects of main process parameters, this study focuses on the sensitivity analysis of parameters and fine tuning requirements of the parameters for optimum weld bead geometry. Changeable process parameters such as welding current, welding voltage and welding speed are used as design variables. The objective function is formed using width, height and penetration of the weld bead. Experimental part of the study is based on three level factorial designs of three process parameters. In order to investigate the effects of input (process) parameters on output parameters, which determine the weld bead geometry, a mathematical model is constructed by using multiple curvilinear regression analysis. After carrying out a sensitivity analysis using developed empirical equations, relative effects of input parameters on output parameters are obtained. Effects of all three design parameters on the bead width and bead height show that even small changes in these parameters play an important role in the quality of welding operation. The results also reveal that the penetration is almost non-sensitive to the variations in voltage and speed.

[2] **Kook-soo Bang et al. [2008]** said that submerged arc welding was performed using metal cored wires and fluxes with different compositions. The effects of wire/flux combination on the chemical composition, tensile strength, and impact toughness of the weld metal were investigated and interpreted in terms of element transfer between the slag and the weld metal, i.e., quantity. Both carbon and manganese show negative quantity in most combinations, indicating the transfer of the elements from the weld metal to the slag during welding. The amount of transfer, however, is different depending on the flux composition. More basic fluxes yield less negative C and Mn through the reduction of oxygen content in the weld metal and presumably higher Mn activity in the slag, respectively. The transfer of silicon, however, is influenced by  $\text{Al}_2\text{O}_3$ ,  $\text{TiO}_2$  and  $\text{ZrO}_2$  contents in the flux. Si becomes less negative and reaches a positive value of 0.044 as the oxides contents increase. This is because Al, Ti, and Zr could replace Si in the  $\text{SiO}_2$  network, leaving more Si free to transfer from the slag to the weld metal.

[3] **Keshav Prasad et al. [2006]** investigated the influence of the submerged arc welding (SAW) process parameters (welding current and welding speed) on the microstructure, hardness, and toughness of Plain carbon steel weld joints. Attempts have also been made to analyze the results on the basis of the heat input. The SAW process was used for the welding of 16 mm thick plain steel plates. The weld joints were prepared using comparatively high heat input (3.0 to 6.3 KJ/mm) by varying welding current (500–700 A) and welding speed (200–300 mm/min). Results showed that the increase in heat input coarsens the grain structure both in the weld metal and heat affected zone (HAZ). The hardness has been found to vary from the weld centre line to base metal and peak hardness was found in the HAZ. The hardness of the weld metal was largely uniform. The hardness reduced with the increase in welding current and reduction in welding speed (increasing heat input) while the toughness showed mixed trend. The increase in welding current from 500 A to 600 A at a given welding speed (200 mm/min or 300 mm/min) increased toughness and further increase in welding current up to 700 A lowered the toughness.

[4] **R Quintana et al. [2003]**, developed metal coatings with complex chemical compositions and phases, as well as differing mechanical properties, the Submerged Arc Welding (SAW) process is often used, employing a great variety of types of agglomerate fluxes<sup>1</sup>. All agglomerate fluxes consist of two fundamental parts: the matrix and the alloyed load. The two constituents of the flux aggregate, by various processes, with the help of agglomerating agents. Agglomeration by granulation (pelletizing) using liquid sodium or potassium glass is the most common and widely used for these types of fluxes. One of the most significant profitability characteristics of an agglomerate flux is the efficiency of the transfer of the chemical element of the alloyed load of the flux to the deposited metal by particular wire–flux systems and welding regimens. The elements of the alloyed load can constitute up to 85% of the production cost of the flux. One of the most widely used and economic alloy systems for fluxes used to refinish pieces subject to wear due to abrasion and light impact, and for metal to metal wear, is the system constituted by FeCr, FeMn and graphite. The chemical activity and structural characteristics of the matrix of the agglomerate flux influence the efficacy of the transfer of the chemical elements alloyed to the metal deposited during SAW. In chemical terms, the SAW process can be considered a very heterogeneous reaction, which develops in different states and ranges of temperature and

concentration, the reacting components of which are wire–electrode, flux and base material. The final product of this reaction is an alloy (welding cord), with a specific chemical composition, microstructure and mechanical properties, which can be modified according to technological parameters, with slag and gases.

[5] **P. Kanjilal et al. [2005]**, had shown rotatable designs based on statistical experiments for mixtures have been developed to predict the combined effect of flux mixture and welding parameters on submerged arc weld metal chemical composition and mechanical properties. Bead-on-plate weld deposits on low carbon steel plates were made at different flux composition and welding parameter combinations. The results show that flux mixture related variables based on individual flux ingredients and welding parameters have individual as well as interaction effects on responses, viz. weld metal chemical composition and mechanical properties. In general, two factor interaction effects are higher than the individual effect of mixture related variables. Amongst welding parameters, polarity is found to be important for all responses under study.

[6] **J. Tuseka et al. [2003]**, studied multiple-wire submerged-arc welding and cladding with metal-powder addition. Three different ways of supplying the metal powder to the welding area are described and shown schematically. It was found that the use of metal powder will increase the deposition rate and the welding-arc efficiency and reduce the shielding-flux consumption. A suitable device permits submerged-arc welding and cladding with metal-powder addition. The process is primarily meant for the cladding of worn surfaces or the production of surfaces with certain characteristics (corrosion or wear resistance). By using the metal-powder addition it is possible to alloy a weld or a cladding with optional chemical elements.

[7] **R. S. Chandel et al. [1998]**, suggested that conventional submerged arc welding (SAW) process has a very high deposition rate, there has been continued effort in further improving that rate. Consequently, many variants of SAW multiple wire, strip electrodes etc., are now available and widely used for specific applications. With the use of proper parameters and SAW variant, it is now possible to achieve deposition rates in excess of 50 kg/hr. The increase in deposition rate in most cases is, however, achieved by increasing welding current and hence the heat input, which tends to impair joint toughness. The mechanical properties,

particularly the toughness of high heat input welds, are known to be inferior due to grain coarsening in the heat-affected zone (HAZ) and segregation and large columnar grains in the weld metal. Thus, the increase in deposition rate by increasing heat input is at the expense of mechanical properties. This factor is becoming more and more important due to the emergence of high-strength materials such as high strength low alloys. Many researchers have shown that by adding the powder in SAW, a better use of heat can be made; thus, for a given heat input, the number of passes required to a joint can be reduced and, therefore, the total energy supplied to the joint can be reduced. Alternatively, the same bead size or deposition rate can be achieved by lowering heat input per pass. Welds made with lower heat input experience higher cooling rates, and thermal gradients are steeper; hence, the width of the HAZ is also less. Additionally, the time spent above the peak temperature is reduced; the combined effect of this results in a narrow HAZ that cools faster and has smaller grain growth. Weld metals produced under faster cooling rates are also superior in mechanical properties. Thus, the process of powder addition has potential not only for producing welds that are cost effective but metallurgical superior, too, and they may become attractive for welding plain carbon steel. In light of this, a study was carried out to evaluate the effect of the addition of metal powder on the mechanical properties of SAW metal made in steel.

**[8] Saurav Datta et al. [2006]** said that quality has now become an important issue in today's manufacturing world. Whenever a product is capable of conforming to desirable characteristics that suit its area of application, it is termed as high quality. Therefore, every manufacturing process has to be designed in such a way that the outcome would result in a high quality product. The selection of the manufacturing conditions to yield the highest desirability can be determined through process optimization. Therefore, there exists an increasing need to search for the optimal conditions. In the present work, we aim to evaluate an optimal parameter combination to obtain acceptable quality characteristics of bead geometry in submerged arc bead-on-plate weldment on mild steel plates. The SAW process has been designed to consume fused flux, in the mixture of fresh flux. Thus, the work tries to utilize the concept of 'waste to wealth'. Apart from process optimization, the work has been initiated to develop mathematical models to show different bead geometry parameters, as a function of process variables. Hence, optimization has been performed to determine the maximum amount of slag-flux mixture that can be used without sacrificing any negative

effect on bead geometry, compared to the conventional SAW process, which consumes fresh flux only. Experiments have been conducted using welding current, slag-mix percentage and flux basicity index as process parameters, varied at four different levels. Using four 3 full factorial designs, without replication, we have carried out welding on mild steel plates to obtain bead-on plate welds. After measuring bead width, depth of penetration and reinforcement; based on simple assumptions on the shape of bead geometry, we calculated other relevant bead geometry parameters: percentage dilution, weld penetration shape factor, weld reinforcement form factor, area of penetration, area of reinforcement and total bead cross sectional area.

**[9] T.W. Eagar [1979]** studied the sources, mechanism and expected levels of oxygen and nitrogen contamination during gas-tungsten arc welding, gas metal arc, shielded metal arc, self-shielded-metal arc welding and submerged arc welding are reviewed. The importance of decomposition of  $\text{Si}_2\text{O}$  into silicon monoxide and oxygen were presented, indicating that silicon transfer between the slag and metal occurs by a gas-metal rather than a slag-metal reaction mechanism.

**[10] P.H Tiwari [1979]** studied the erosion corrosion of carbon steel in aqueous  $\text{H}_2\text{S}$  solutions up to 120 degree Celsius and 1.6MPa Pressure by rotating disc technique. It was found that the loss of iron from carbon steel disc increases with the speed of the rotation. The amount of iron sulfide ( $\text{H}_2\text{S}$ ) adhering to the carbon steel (the scale) remains the same at different speed of rotation, as fresh layer of iron sulphide (mackinawite) replaces the almost instantaneously. Fluid velocity was found to affect the nature of the film of iron sulfide formed on the carbon steel surfaces exposed to  $\text{H}_2\text{S}$  solutions.

**[11] Behcet Gulenc et al. [2003]** said that submerged arc welding process is commonly used due to its easy applicability, high current density and its ability to deposit a large amount of weld metal using more than one wire at the same time, especially in restoration of worn parts, which is of great importance to manufacturers. In this study, worn parts were welded using the submerged arc welding process. Various wires and fluxes were used for this purpose. These welded parts were subjected to wear tests under different loads, and changes in the hardness and microstructures were examined. The results showed that the hardest weld metal showed the highest wear resistance, while the least hard weld metal showed the least

wear resistance. The weld hardness and wear resistance obtained were found to be dependent on the chemical composition of the weld wire and flux.

**[12] C.S. Chai and T.W. Eagar [1981]** both investigated Slag Metal Reactions in Binary  $\text{CaF}_2$ -Metal oxide Welding Fluxes. Stability of metal oxides commonly used in welding fluxes was studied by producing binary  $\text{CaF}_2$ -Metal oxide fluxes. The oxides investigated include Silicon oxide, manganese oxide, aluminum oxide, nitrogen-oxide and calcium oxide. The results showed that some chemically stable fluxes may decompose into sub oxides in the presence of welding arcs, thereby providing higher levels of oxygen in weld metal than those oxides which do not form sub oxides. A study of oxygen, silicon and manganese recovery in binary  $\text{Ca}_2\text{F}$ -metal oxides fluxes has shown that calcium fluoride reduces the oxidizing potential of welding fluxes, although the reason for the reduction is probably due to dilution of the reactive oxides by the  $\text{Ca}_2\text{F}$  rather than to reactivity of the calcium fluoride itself.

**[13] J. I. Federer [1983]** studied the Corrosion of Fluidized-Bed Boiler Materials in Synthetic Flue Gas. Candidate materials for components of a fluidized-bed waste heat recovery system (FBWHRS) include plain carbon steel, types 405 and 316 stainless steel, and alloy 800. These materials were exposed to synthetic flue gas at anticipated FBWNRS temperatures and higher for 3000 h to determine corrosion rates. The synthetic flue gas was a combustion atmosphere to which  $\text{Cl}_2$  and  $\text{HCl}$  were added. The projected annual corrosion rate for plain carbon steel was about 0.08mm/year (0.003 in/year) at 250 to 290°C, but it would exceed 0.5 mm/year (0.02in./year) at 560°C. The projected annual corrosion rate of other materials were less than 0.25m/year (0.01in/year) at the maximum test temperatures of 560,660, and 665°C for type 405, type 316, and alloy 800, respectively. These results indicated that corrosion of candidate FBWHRS materials would not be significant at anticipated operating temperatures for various components unless other factors, not included in this study, cause accelerated corrosion.

**[14] Katsuhisa Sugimoto [1990]** studied the influence of environmental factors on the corrosion and the corrosion behavior of carbon steel by aqueous sulfide have been examined by using the weight loss of specimens in immersion tests and electro-chemical methods. The possibility of corrosion monitoring by electrode-impedance measurement has been examined. Experiments were conducted with sulfide, chloride and ammonia concentrations

b/w 10 and 1500ppm, a pH range b/w 3 and 10, a temp. between 25 & 90 degree C, and a fluid velocity between 0 and 3.0 m/s. The corrosion behavior of steel was found to depend on pH value, the corrosion rate of carbon steel increases with increasing temperature and fluid velocity. In this paper the influence of environment factors on the corrosion are found by static and dynamic immersion test and following conclusions were found: The corrosion behavior of carbon steel in sour environment depend upon the pH value. In acid solutions below pH 4, the corrosion is high owing to high concentration of hydrogen ions, which promotes iron dissolution. In neutral solution of pH value of 4 and 8, corrosion maxima appear b/w pH 6 and 7 because the iron sulfide film of mackinawite on the specimen is less protective. In alkaline solutions above pH 8, a protective film of Troilite is formed on the specimen, corrosion rate of carbon steel increases with increasing temperature and fluid-flow velocity. The corrosion rate was found to increase by the sulfide concentration but not so much by Chloride and ammonia concentrations.

**[15] U. Mitra and T.W Eagar [1991]** developed the kinetic model to describe the transfer of alloying elements between the slag and metal during flux-shielded welding. The model accounts for changes in alloy recovery based on the geometry of the resulting weld bead. It also distinguished the compositional differences between the single-pass and multi-pass welds beads. It is also shown that the final weld metal oxygen content is directly related to the weld solidification time as well as the type of flux used. Experiments demonstrated that widely held droplet reaction theory cannot explain the transfer of alloying elements between the slag and the metal. It is found that the chemical interaction between slag and metal occur in three zones; the zone of droplet reactions, zone of dilution and weld pool reactions and zone of cooling and solidifying weld pool.

**[16] D.L. Olson et al. [1993]** discussed various aspects of corrosion failures of for different filler materials and other welding conditions. K.N. Choo, Y.H. Kang, S.I. Ryun et. al [21] studied the influence of Nb content and heat treatment on the structure and isothermal corrosion behavior of Zr-Nb alloys at 300, 360 and 400°C in static heavy water and steam (1500 psi) are presented. The formation of the martensitic  $\alpha'$ -phase by  $\beta$ -quenching treatment results in high weight gains at all test temperatures. Up to 5 wt% Nib, the corrosion resistance of the quenched alloy decreases linearly with increasing Nib content.

The Zr-2.5% Nib alloy is used as a pressure tube material for CANDU-PHW reactors and Zr-1% Nib alloy is used as the primary cladding material in Soviet WER-type PWR reactors. Because of their good mechanical and corrosion properties, Zr-Nb alloys have been studied as candidate materials for improved fuel cladding. The corrosion resistance of Zr-Nb alloys in aqueous and gaseous media is sensitive to, among other factors, the microstructure which in turn is influenced by Nib concentration and heat treatment. The structural changes produced by the variation in Nib concentration and heat treatment have been investigated by many workers.

**[17] F. Kadirgan and S. Suzer [2001]** studied the corrosion behavior of a new inhibitor (FT2000) in saline solution on alloy carbon steel in the neutral aqueous media at 60°C. Effect of sulfate ion is also studied. Corrosion rate, polarization resistance, and efficiency of the inhibitor were calculated. The nature of the protecting layer formed in the presence of the inhibitor is investigated by X-ray photoelectron spectroscopy, XPS.

**[18] Y.F. Cheng and F.R. Steward [2004]** used the electrochemical methods to study the corrosion behavior of five Fe–Cr alloy steels and 304L stainless steel in high-temperature water. Passivity could be achieved on A-106 B carbon steel with a small content of chromium, which could not be passivity at room temperature. The formation rate and the stability of the magnetite films increased with increasing Cr content in the steels.

**[19] P. Bala Srinivasan et al. [2006]** studied the effect of impact strength and corrosion behavior of shielded metal arc welded dissimilar weldments between UNS 31803 and IS 2062 steels with E2209 and E309 electrodes. The hardness and impact strength of the weld metal produced with E2209 electrodes were found to be better than that obtained with E309. Though the general corrosion resistance of the weld metal produced with E309 was superior in 1M NaCl solution, they exhibited a higher pitting susceptibility in this test environment. The passivation behavior of the weld metal with E2209 was observed to be on par with that of the duplex stainless steel base material (DSSBM) in Hydro sulfuric solution: however, in terms of pitting resistance in 1M NaCl solution both weld metals were inferior to DSSBM. Though E309 electrodes are widely employed for producing dissimilar weld joints, based on the observations in the current work, it is concluded that the E2209 electrode is the most suitable consumable for joining Dissimilar Duplex stainless steel(DSS) to Carbon Steel(CS).

[20] **P. Yayla, E. Kaluc et al. [2007]** studied Effects of welding processes on the mechanical properties of HY 80 steel weldments. Different welding techniques were used in this study to evaluate the mechanical performance of weldments of HY-80 steel. Weldments were prepared using different welding processes such as shielded metal arc welding, gas metal arc welding, and submerged metal arc. The objective was to determine the optimum welding method for the steel. After welding, the effects of welding methods on weld metal microstructure and mechanical properties including weld metal tensile strength and Charpy V-notch impact toughness over the temperature range of -20 to 20 deg C are investigated. Charpy impact and tensile tests were performed on standard notched specimens obtained from the welded and main sections of the material. The hardness distribution measurements on the differently welded specimens are conducted in order to gain a deep insight of different welding methods.

[21] **P. Kanjilal, T.K. Pal and S.K. Majumdar [2006]** presented the statistical experiments for mixtures, to predict combined the effect of flux and welding parameters on chemical composition and mechanical properties of submerged arc weld metal. Bead on plate weld deposits on low carbon steel plates were made at different flux composition and welding parameters combinations. The results show that flux mixture related variables based on individual flux ingredients and welding parameters have individual as well as interaction effects on responses, viz. weld metal chemical composition and mechanical properties. Recent studies involving SAW of carbon and carbon-manganese steels have generated data for both commercial and experimental fluxes from which composition of weld metal can be predicted for a given flux, wire and base plate.

[22] **S.P Kumaresh Babu and S .Natranjan [2007]** studied welding plays an essential role in fabrication of components such as boiler drum, pipe work, heat exchangers, etc. used in power plant. Gas tungsten arc welding (GTAW) is mainly used for welding of boiler components. Pulsed GTAW is another process widely used where high quality and precision welds are required. In all welding processes, the intense heat produced by the arc and the associated local heating and cooling lead to varied corrosion behavior and several metallurgical phase changes. Electrochemical polarization techniques such as Tafel line

extrapolation (Tafel), linear polarization resistance (LPR), and ac impedance method have been used to measure the corrosion current.

**[23] S.P Kumaresh Babu and S. Natranjan [2007]** carried out an experimental work to evaluate and compare corrosion and its inhibitor in SA 516 Gr. 70 carbon steel boiler weldments made by Submerged arc welding process with four different heat inputs exposed to hydrochloric acid medium at 0.1M, 0.5M and 1.0M concentration. Electrochemical Polarization techniques such as Tafel line extrapolation and Linear Polarization resistance have been used to measure the corrosion current. The role of hexamine and mixed inhibitor, each at 100ppm concentration is studied in these experiments.

**[24] S.P Kumaresh Babu and S. Nataranjan [2010]** studied the high temperature corrosion and characterization studies in Flux Cored Arc Welded 2.25Cr-1Mo power plant Steel. Higher productivity is registered with flux cored arc welding (FCAW) process in many applications. It combines the characteristics of SMAW, GMAW and SAW processes. This paper describes the experimental work carried out to evaluate and compare corrosion and its inhabitation in SA 387 Gr.22 (2.25Cr-1Mo) steel weldmets prepared by FCAW process with four different heat inputs exposed to hydrochloric acid medium at different concentration levels. Electrochemical polarization techniques such Tafel line extrapolation and linear polarization resistance have been used to measure the corrosion current.

**[25] D.J. Lee K.H. et al. [2009]** studied the pitting corrosion behavior on welded joints of AISI 304L austenitic stainless steel was investigated with the flux-cored arc welding (FCAW) process. The dependence of pitting corrosion susceptibility on the microstructure and constituents was compared in weld metals by using three newly designed filler wires. Mechanical examination demonstrated that the tensile and yield strengths were increased with increasing equivalent weight ratio of chromium/nickel ( $C_{req}/N_{ieq}$ ). Ductility-dip cracking (DDC) was observed in the fully austenitic structure in the deposited metal, and it detrimentally affected the pitting resistance. Potentiodynamic anodic polarization results revealed that the passive film breakdown was initiated in the crack opening, and that the concentration of chloride ions and corrosion products induced severe damage near to the DDC.

[26] **N. A. Mcpherson et al. [1998]** produced Butt welds using the submerged arc welding (SAW) process to join a carbon steel plate of normal shipbuilding grade to an austenitic stainless steel plate. Variables used in this work were the position of the consumable wire in the weld preparation and the ferrite number of the consumable wire. Abnormally high hardnesses were measured in some regions of the welds. These were related to the central position of the consumable wire in the weld preparation. Undesirably low ferrite numbers were related to the ferrite number of the consumable wire and also to the central position of the consumable wire in the weld preparation. The position of the consumable wire in the weld preparation controlled the relative dilution from the parent plates, and when the dilution from the 316LN steel was increased by off-setting the wire to that side of the weld preparation, the high hardness regions were no longer found. Similar optical microstructures were found to have significantly different hardnesses, which were related to the dilution effects, which were also related to the wire position within the weld preparation.

[27] **Vera Lu et al. [2001]** carried out Post weld heat treatment (PWHT) is frequently applied to steel pressure vessels, following the requirements of the ASME code, which establishes the parameters of the PWHT based on the thickness and chemical composition of the welded section. This work shows the results of an analysis undertaken on a sample of ASTM A537 C1 steel subjected to qualifying welding procedure tests including PWHT. The results obtained showed that this PWHT practice promoted a reduction in the mechanical properties of the base metal and the heat-affected zone (HAZ).

[28] **Abilio Manuel et al. [2007]** introduced normalized fine grain carbon low alloy steel, P355NL1, intended for service in welded pressure vessels, where notch toughness is of high importance, has been investigated. Applications with this steel usually require the intensive use of welds. One of the most common welding processes that are used in the manufacturing of pressure vessels is the submerged arc welding. This welding process is often automated in order to perform the main seam welds of the body of the vessels. The influence of the automated submerged arc welding, in the mechanical performance, is investigated. The low and high cycle fatigue and crack propagation behaviors are compared between the base and welded materials. Several series of small and smooth specimens as well as cracked specimens made of base, welded and heat affected materials, respectively, were fatigue

tested. Strain, stress and energy based relations for fatigue life assessment, until crack initiation, are evaluated based on experimental results and compared between the base and welded materials. Finally, the fatigue crack propagation behaviors are compared between the base, welded and heat affected materials

**[29] Saurav Datta et al. [2009]** discussed optimization problem of submerged arc welding. The target was to search an optimal process environment, capable of producing desired bead geometry parameters of the weldment. Four correlated features of bead geometry: depth of penetration, reinforcement, bead width, and percentage dilution has been selected in the study. The process environment has been assumed consisting of variables like voltage, wire feed rate, traverse speed. Multiple correlated responses have been converted into independent quality indices called principal components. Principal component analysis (PCA) has been adapted to covert multiple objectives of the optimization problem into a single objective function. This single objective function has been denoted as composite principal component. Taguchi's robust optimization technique has been applied to determine the optimal setting, which can maximize the composite principal component. Result of this aforesaid optimization technique has been compared to that of grey- Taguchi technique; another approach which is widely used for solving multi criteria optimization problems. A confirmatory test showed satisfactory result.

**[30] H.S. Moon et al. [2002]** investigated significant portion of the total manufacturing time for a pipe fabrication process is spent on the welding following the primary machining and fit-up processes. To achieve a reliable weld bead appearance, automatic seam tracking and adaptive control to fill the groove are urgently required. For seam tracking in the welding processes, vision sensors have been successfully applied. However, the adaptive filling control for a multi torch system for the appropriate welded area has not yet been implemented in the area of submerged arc welding (SAW). This describes several advances in sensor and process control techniques for applications in SAW which combine to give a fully automatic system capable of controlling and adapting the overall welding process. This technology has been used in longitudinal and spiral pipe mills and in pressure vessel production.

[31] **BY E. Baune et al. [2000]** perform the experiment using a set of five experimental FCAW electrodes, an improved version of the basicity index formula is developed. This new methodology is described in two papers, titled Part 1: Solidified Slag Composition of a FCAW Consumable as a Basicity Indicator and Part 2: Verification of the Flux/Slag Analysis Methodology for Weld Metal Oxygen Control. To accomplish this purpose, the partition of the various elements contained in the formulation of one FCAW electrode is studied and modeled in Part 1. Correspondingly, the composition of the solidified slag is predicted for this particular electrode. To verify the model, the prediction of the slag chemical composition is compared with experimental measurements. Good accordance is found, which shows the model is applicable. A new way of defining the basicity of a FCAW consumable based on the chemical composition of the slag is derived. In Part 2, comparison of this innovative methodology with formula is achieved, as well as with other means reported in the literature for expressing the flux/slag basicity. The newly defined basicity index is found to offer superior correlation with the weld metal oxygen content, demonstrating the validity of the assumptions made in the present investigation.

[32] **Saurav Datta et al. [2006]** carried out application of the Taguchi method in combination with grey relational analysis has been applied for solving multiple criteria (objective) optimization problem in submerged arc welding (SAW). A grey relational grade evaluated with grey relational analysis has been adopted to reveal an optimal parameter combination in order to obtain acceptable features of weld quality characteristics in submerged arc bead-on-plate welding. The idea of slag utilization, in subsequent runs, after mixing it with fresh un melted flux, has been introduced. The parentage of slag in the mixture of fresh flux and fused flux (slag) has been denoted as slag-mix percentage. Apart from two conventional process parameters: welding current and flux basicity index, the study aimed at using varying percentages of slag-mix, treated as another process variable, to show the extent of acceptability of using slag mix in conventional SAW processes, without sacrificing any characteristic features of weld bead geometry and HAZ, within the experimental domain. The quality characteristics associated with bead geometry and HAZ were bead width, reinforcement, depth of penetration and HAZ width. Predicted results have been verified with confirmatory experiments, showing good agreement. This proves the utility of the proposed method for quality improvement in SAW process and provides the

maximum (optimum) amount of slag-mix that can be consumed in the SAW process without any negative effect on characteristic features of the quality of the weldment in terms of bead geometry.

**[33] Vinod Kumar et al. [2009]** suggested that submerged arc welding contributes to approximately 10% of the total welding. Approximately 10% -15% of the flux gets converted into very fine particles termed as flux dust before and after welding, due to transportation and handling. If welding is performed without removing these very fine particles from the flux, the gases generated during welding are not able to escape, thus it may result into surface pitting (pocking) and even porosity. On the other hand, if these fine particles are removed by sieving, the cost of welding will be increased significantly. And if this flux dust is dumped/ thrown, will create the pollution. Therefore to reduce the cost of welding and pollution, in the present work attempts have been made to develop the acidic and basic agglomerated fluxes by utilizing wasted flux dust. The investigation of the present study showed chemical composition and mechanical properties of the all weld metal prepared from the developed fluxes and the parent fluxes to be in the same range. The welded joints were also found to be radio graphically sound. Therefore the developed fluxes prepared from the waste flux dust can be used without any compromise in mechanical properties and quality of the welded joint. It will reduce the cost of welding and pollution

The problem was to study the corrosion behaviour of Structural steels welds by development of different kinds of fluxes by submerged arc welding. Structural steel used for welding having carbon percentage 0.24 with SA 70 grade. The corrosion behaviour, corrosion rate and the change in physical and mechanical properties were also being taken into consideration. For the achievement of the above, an experimental set up was prepared where all the necessary inputs were made. The aim of the experiment was to study the effect of fluxes on the corrosion resistance of submerged arc elements or development of submerged arc welding fluxes for enhanced corrosion resistance of Structural steel welds. The experiment was carried out by preparing the samples of required material and size by submerged arc welding.

### **3.1 Objectives**

1. Development of submerged arc welding fluxes for enhanced corrosion resistance of structural steel welds.
2. To study the effect of different fluxes on micro hardness, microstructure, composition, tensile strength and impact test etc.

Extensive tests were carried out using the Submerged Arc Welding Machine to achieve the objective of minimizing the corrosion rate by using appropriate selection of material and welding consumables etc. The following are the steps which were followed to achieve the objective:

- (a) *Preparation of flux*: For the manufacturing of flux for SAW, various compounds such as CaF<sub>2</sub>, CaO, MnO, SiO<sub>2</sub>, Al<sub>2</sub>O<sub>3</sub>, TiO<sub>2</sub> etc. were used.
- (b) *Method of preparation of steel plate specimen*: To prepare the steel plate specimens, steel plate of dimension 250x125x12 mm was used. After cutting of plates a V joint 60 degree angle was made. Tacking was done on the back side of the plates, to avoid leveling mistake while doing SAW.
- (c) After performing SAW operation, the specimens were cut from the welded plate to carry out various tests.

The following are the tests carried out to achieve the objective:

- Corrosion Rate
- Tensile Test
- Toughness Test
- Micro Hardness, Microstructure etc.

Table 4.1 shows the test matrix in which parameters variation is given.

**Table 4.1: Test Matrix**

RUN 1				RUN 2			
Welding Flux	Current (A)	Voltage (V)	Travelling speed (m/h)	Welding Flux	Current (A)	Voltage (V)	Travelling speed (m/h)
1	350	32	28	1	400	34	26
2	350	32	28	2	400	34	26
3	350	32	28	3	400	34	26
4	350	32	28	4	400	34	26
5	350	32	28	5	400	34	26
6	350	32	28	6	400	34	26
7	350	32	28	7	400	34	26

## 4.1 METHOD OF PREPARATION OF FLUX

For the manufacturing of flux, 7 different compounds viz., CaF<sub>2</sub>, CaO, Na<sub>2</sub>O, MnO, SiO<sub>2</sub>, Al<sub>2</sub>O<sub>3</sub>, TiO<sub>2</sub> were used. The compounds were received in powder form and mixed together (manually) with binder (Sodium Silicate) in different weight percentages to prepare the required type of flux. Fluxes are of two types viz., acidic and basic. To prepare the basic flux basicity index was calculated shown below.

$$B.I = \frac{CaF_2 + CaO + Na_2O + 0.5(MnO + FeO)}{SiO_2 + 0.5(Al_2O_3 + TiO_2 + ZrO_2)}$$

The following table 4.2 to 4.8 shows the weight of constituents in grams to prepare the flux of required chemical compositions.

**Table 4.2: Chemical composition of Flux 1:**

S. No	Flux Constituent	Weight of constituent (gm)
1	CaO	10
2	MnO	5
3	Silica	5
4	Fly Ash	5
5	Al <sub>2</sub> O <sub>3</sub>	10
6	TiO <sub>2</sub>	15
7	Iron Powder	2
8	Sodium Silicate (Binder)	20
9	CaF <sub>2</sub>	20
10	Cr <sub>2</sub> O <sub>3</sub>	5
11	KF	5

**Table 4.3: Chemical composition of Flux 2:**

S. No	Flux Constituent	Weight of constituent (gm)
1	CaO	5
2	MnO	1
3	Silica	15
4	Fly Ash	15
5	Al <sub>2</sub> O <sub>3</sub>	10
6	TiO <sub>2</sub>	15
7	Iron Powder	1
8	Sodium Silicate (Binder)	20
9	CaF <sub>2</sub>	10
10	Cr <sub>2</sub> O <sub>3</sub>	5
11	KF	5

**Table 4.4: Chemical composition of Flux 3:**

S. No	Flux Constituent	Weight of constituent (gm)
1	CaO	10
2	MnO	1
3	Silica	15
4	Fly Ash	10
5	Al <sub>2</sub> O <sub>3</sub>	15
6	TiO <sub>2</sub>	15
7	Iron Powder	-
8	Sodium Silicate (Binder)	20
9	CaF <sub>2</sub>	5
10	Cr <sub>2</sub> O <sub>3</sub>	5
11	KF	5

**Table 4.5: Chemical composition of Flux 4:**

S. No	Flux Constituent	Weight of constituent (gm)
1	CaO	15
2	MnO	5
3	Silica	-
4	Fly Ash	5
5	Al <sub>2</sub> O <sub>3</sub>	15
6	TiO <sub>2</sub>	15
7	Iron Powder	2
8	Sodium Silicate (Binder)	20
9	CaF <sub>2</sub>	15
10	Cr <sub>2</sub> O <sub>3</sub>	5
11	KF	5

**Table 4.6: Chemical composition of Flux 5:**

S. No	Flux Constituent	Weight of constituent (gm)
1	CaO	10
2	MnO	5
3	Silica	-
4	Fly Ash	-
5	Al <sub>2</sub> O <sub>3</sub>	15
6	TiO <sub>2</sub>	15
7	Iron Powder	2
8	Sodium Silicate (Binder)	20
9	CaF <sub>2</sub>	30
10	Cr <sub>2</sub> O <sub>3</sub>	5
11	KF	5

**Table 4.7: Chemical composition of Flux 6:**

S. No	Flux Constituent	Weight of constituent (gm)
1	CaO	20
2	MnO	5
3	Silica	5
4	Fly Ash	5
5	Al <sub>2</sub> O <sub>3</sub>	15
6	TiO <sub>2</sub>	15
7	Iron Powder	2
8	Sodium Silicate (Binder)	20
9	CaF <sub>2</sub>	5
10	Cr <sub>2</sub> O <sub>3</sub>	5
11	KF	5

**Table 4.8: Chemical composition of Flux 7:**

S. No	Flux Constituent	Weight of constituent (gm)
1	CaO	10
2	MnO	5
3	Silica	5
4	Fly Ash	10
5	Al <sub>2</sub> O <sub>3</sub>	15
6	TiO <sub>2</sub>	15
7	Iron Powder	1
8	Sodium Silicate (Binder)	20
9	CaF <sub>2</sub>	10
10	Cr <sub>2</sub> O <sub>3</sub>	5
11	KF	5

**Table 4.9: Basicity index**

Flux	1	2	3	4	5	6	7
<b>Basicity Index</b>	1.87	1.16	1.02	1.52	1.96	1.32	1.22

The solution of sodium silicate (20% weight of flux) binder was added to the dry mixed powder (fig.4.2) and it was mixed for 10 min. Sodium silicate was added for better arc stability. The mixture flux were dried in air for 24 h and then baked in the pit furnace at approximate 700°C for nearly 3 h. After cooling, this flux were crushed and sieved to get required size (fig.4.3, 4.4). After sieving, fluxes were kept in air-tight bags so as to keep it free from moisture. By using this method we make 7 different kind of flux.



**Fig. 4.2: Compounds mix with Binder**



**Fig. 4.3: Flux after mixing**



**Fig. 4.4: Test sieve (8 BS, 10 ASTM, 2 mm IS, 2057 micron)**

## **4.2 CHEMICAL COMPOSITION OF ELECTRODE AND BASE METAL**

The following table 4.10 and 4.11 shows the composition of base metal and welding electrode was found by using atomic absorption spectrometer.

**Table 4.10: Chemical Composition of Base Metal**

<b>C</b>	<b>Si</b>	<b>Mn</b>	<b>P</b>	<b>S</b>	<b>Cu</b>	<b>Nb</b>	<b>Ti</b>
0.24	0.26	0.49	0.02	0.01	0.09	0.07	0.008

**Table 4.11: Chemical Composition of Electrode**

<b>C</b>	<b>Si</b>	<b>Mn</b>	<b>P</b>	<b>S</b>	<b>Cu</b>	<b>B</b>
0.05	0.1	0.01	0.02	0.09	0.04	0.005

### 4.3 METOD OF PREPARATION OF STEEL SPECIMEN

Fourteen plates of dimension 250x125x12 mm were used for welding. V groove was made at 60 degree angle for the joining of plates. On the back side of the plate tacking (fig.4.5) was done to avoid the misalignment of the plates.



**Fig. 4.5: Tacking on back side of plates**

After tacking, specimen was kept under electrode on flat plate [fig 4.6 (b)] for welding as shown in fig [4.6 (a)] of SAW machine, clamp the specimen with base plate using clampers then by putting 7 different kind of flux one by one in hopper welding was done in V grooves of 7 plates.



(a)



(b)



**Fig: (c)**

**Fig. 4.6: Submerged Arc Welding of Plates**

Fig shows (c) the welding bead on the steel plate after the removal of flux from the weld region. Cut the specimen in required dimension for Corrosion, Tensile test, Toughness, Micro hardness, Microstructure, and Chemical composition.

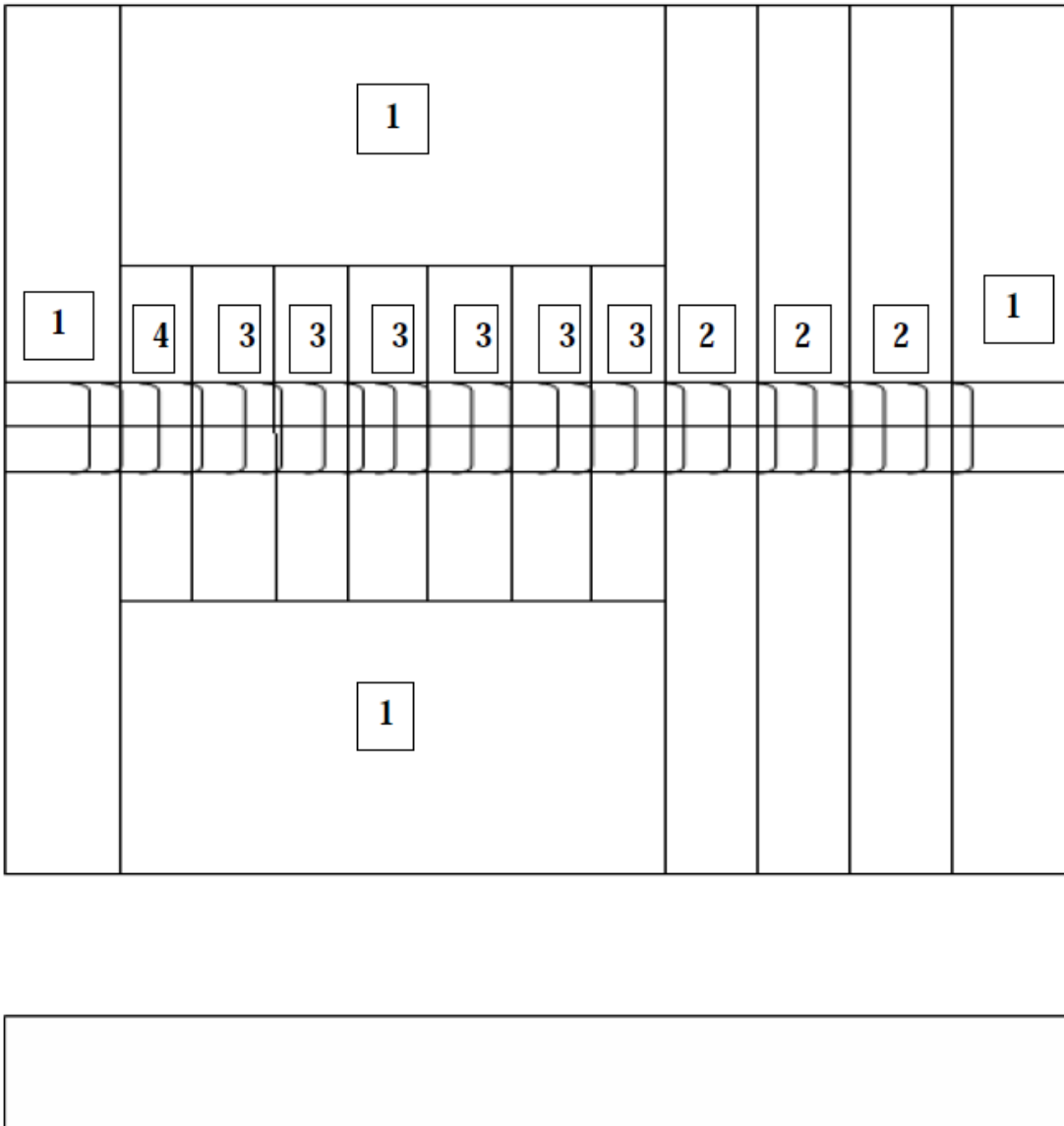


**Fig. 4.7: Cutting of plates after welding**

Orientation of cutting of specimens after welding is shown in fig 4.10, (1) represent waste material, (2) represent tensile test specimen, (3) represent toughness test specimen, (4) represent microstructure, micro hardness, corrosion and composition test specimen.



**Fig. 4.8: Cutting of Plates according to required size, Surface Grinder Machine**



**Fig. 4.9: Cutting of Plates according to required size**



**Fig. 4.10: Plates after grinding from weld area**

Fig. 4.8-4.10 shows the removal of welding bead from the welded plate by grinding operation to make the specimens ready for testing.

## 4.4 TESTING OF WELDED SPECIMENS:

### 4.4.1 Corrosion Testing

The electrodes used for corrosion studies were cut from the submerged arc weld product having dimensions 30 mm x 15mm x 5 mm (l x b x t). They were polished using 100 grit silicon carbide paper followed by 220, 400, 600 and 1000 grades of emery paper, degreased with acetone and rinsed with deionised water (Fig. 4.11). The electrochemical measurements were performed using a potentiostat/frequency response analyzer (ACM instruments, UK) and a flat cell. A 3.5% NaCl solution was used as the electrolyte. Only 1 cm<sup>2</sup> of the sample was exposed to the electrolyte solution.



**Fig. 4.11: Specimens before Corrosion Test**

A graphite rod and saturated calomel electrode (SCE) served as the counter and reference electrodes respectively. All experiments were performed at room temperature. Potentiodynamic polarization measurements were made at a potential scan rate of 60 mV/min. The corrosion potential ( $E_{corr}$ ) and corrosion current density ( $i_{corr}$ ) were determined using the Tafel extrapolation method. Electrochemical impedance (EIS) studies were carried out in the frequency range between 10,000 Hz and 0.01 Hz.

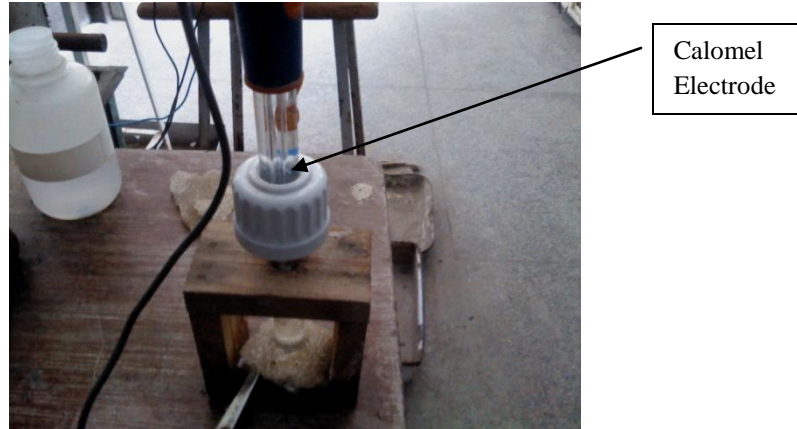


**Fig. 4.12 Saturated calomel electrode (SCE) served reference electrode**

#### 4.4.2 Tensile Test

Ratio of the maximum load a material can support without fracture when being stretched to the original area of a cross section of the material. When stresses less than the tensile strength are removed, a material completely or partially returns to its original size and shape. As the stress approaches that of the tensile strength, a material that has begun to flow forms a narrow, constricted region that is easily fractured. Tensile strengths are measured in units of force per unit area. Universal testing machine was used to find the values of Ultimate Tensile Strength, load vs. displacement and stress vs. strain graphs. Specimens were cut according to the standard size given in fig 4.13.

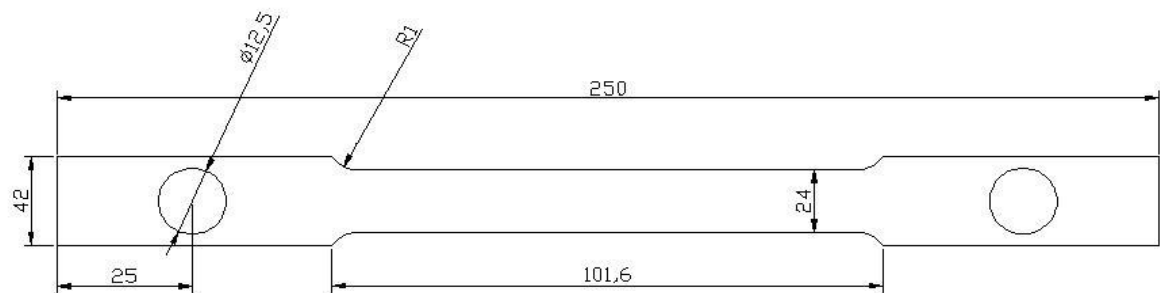


**Fig. 4.13: Orientation of a typical tensile test specimen as per E8M-2008 standard**



**Fig. 4.14: Specimens used for Tensile Testing**

Fig. 4.14 shows the specimens prepared according to the standard size for tensile testing.

#### 4.4.3 Impact Toughness Test

The ability of a metal to rapidly distribute within itself due to both the stress and strain caused by a suddenly applied load or the ability of a material to withstand shock loading. It is the exact opposite of "brittleness" which carries the implication of sudden failure. A brittle material has little resistance to failure once the elastic limit has been reached. According to standard shown in fig. 4.15, Twenty one specimens (Fig. 4.16) were made (3 from each plate) of dimension 10x10x55 mm.

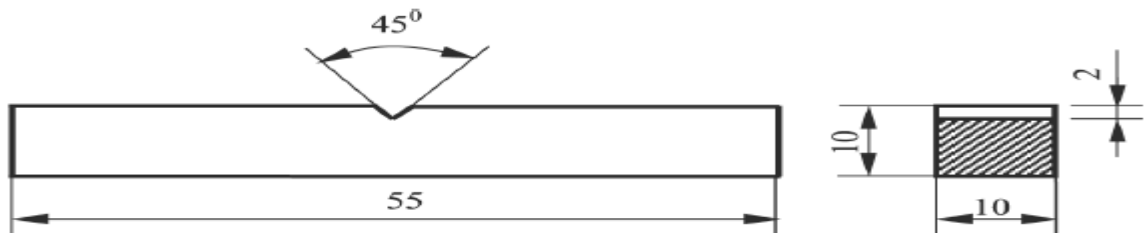


**Fig. 4.15: Standard Charpy test specimen**



**Fig. 4.16: Specimens used for Impact Testing**

#### 4.4.4 Microstructure

A microscope is an instrument to see objects too small for the naked eye. The technology of investigating small objects using such an instrument is called microscopy. Microscopic means invisible to the eye unless aided by a microscope. Many types of microscopes are available but the most common used is the optical microscope which uses light to image the sample. In this test the specimen after cutting rubbed with emery papers of size no. 100, 200, 400, 600, 800, 1000 as shown in Fig. 4.17.

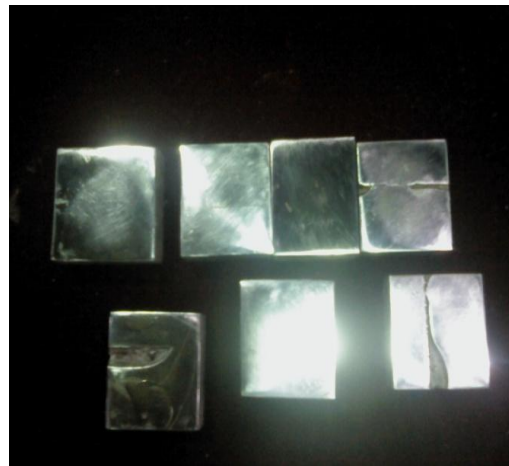


**Fig. 4.17: Pieces for Microstructure & Micro hardness**

#### 4.4.5 Micro Hardness

Micro hardness testing machine was used for measuring the hardness of a material on a microscopic scale. A precision diamond indenter is impressed into the material at loads from a few grams to 1 kilogram. Constant load of 300gm was used for all specimens. The impression length, measured microscopically. The hardness values obtained are useful indicators of a material's properties.

#### 4.4.6 Chemical Composition of Weld Metal

The composition of base metal and welded metal was found by using atomic absorption spectrometer.

#### 4.4.7 Scanning Electron Microscope (SEM)

Scanning electron microscope (SEM) is very important for micro structural analysis. The micro structural characteristic of the sample are used to correlate the effect of different

processing condition with properties and behavior of materials that involves their micro structural changes. SEM provides information relating to topographical features, morphology, phase distribution, compositional differences, crystal orientation and presence of defects and their location.

**5.1 IMPACT TOUGHNESS TEST**

Specimens after impact toughness test carried out at room temperature is shown in fig 5.1



**Fig. 5.1: Specimens after Impact Testing**

**Table 5.1: For Impact Toughness Values**

Basicity Index	Charpy Test (joule)	Average (joule)
Base metal	85+60+75/3	80
1.87	78.48+68.67+68.67/3	71.61
1.16	39.42+29.43+19.62/3	29.43
1.02	19.62+24.52+9.81/3	15.69
1.54	58.86+68.67+78.48/3	68.67
1.96	98.1+98.1+88.29/3	94.17
1.32	49.05+58.86+68.67/3	58.86
1.22	39.42+29.43+19.62/3	29.43

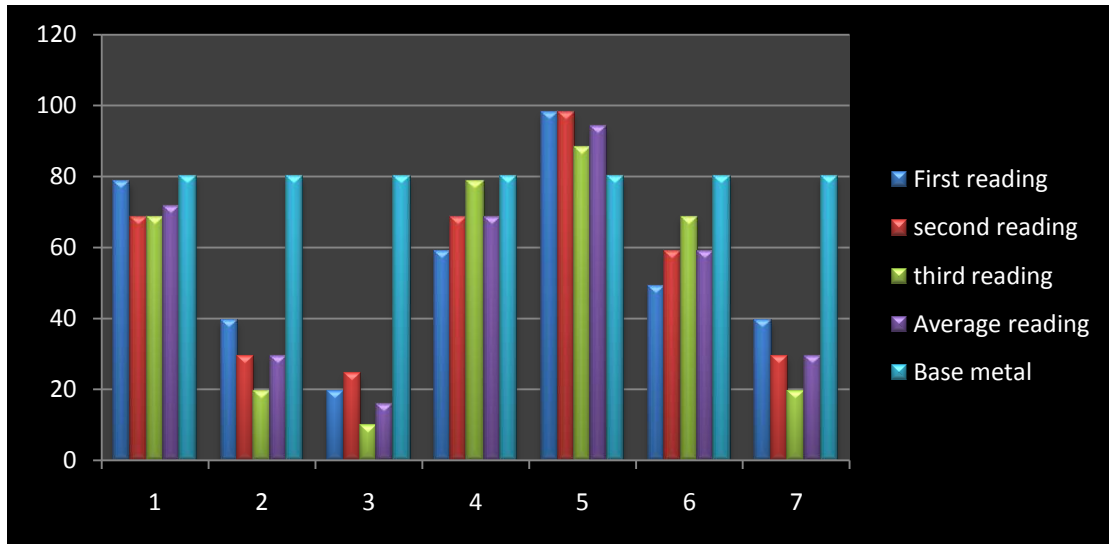


**Fig. 5.2: Graph for Impact Toughness**

### Discussion of Impact Toughness

Results of impact toughness tests for each specimen and average impact toughness values of base material & weld metals at room temperature are shown in table 5.1. It is clear from the Fig. 5.2 that Charpy impact toughness increases with the increase in basicity index. There are several factors affecting the impact toughness of the welds including hardness level, microstructure, percentage of martensite-austenite constituent etc. In all the specimens average value of impact toughness is lower than that of base metal values except flux 5. This is due to the reduced amount of oxygen in the weld metal because of  $\text{CaF}_2$  which acts as a deoxidizer results in increased impact toughness.

## 5.2 CORROSION TESTING

### 5.2 (a) Corrosion Test by Polarization Scan

Specimens after corrosion test by polarization scan method is shown in Fig. 5.3:

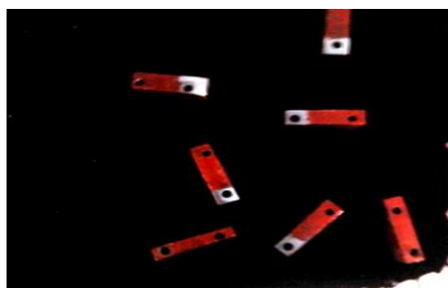


**Fig. 5.3: Specimens after Corrosion Test by Polarization Scan**

The corrosion potential ( $E_{\text{corr}}$ ) and corrosion current density ( $I_{\text{corr}}$ ) calculated using Linear Polarization Resistance (LPR) method is given in table 5.2

**Table 5.2: For Corrosion Rate by Polarization Scan**

S. No	Basicity Index	Corrosion Potential Values(mv) ( $E_{\text{corr}}$ )	Corrosion Current Values( $\mu\text{A}$ ) ( $I_{\text{corr}}$ )	Beta A Values (V/decade)	Beta C Values (V/decade)	Corrosion Rate (mpy)
Base Metal		-589.0	19.00	71.20	164.0	87.42
1	1.87	-632.0	2.590	111.8	97.50	11.88
2	1.16	-671.0	14.10	55.70	92.20	64.57
3	1.02	-690.0	14.30	74.30	100.1	65.66
4	1.54	-659.0	1.960	18.90	18.30	9.002
5	1.96	-683.0	17.00	87.90	109.90	78.18
6	1.32	-685.0	16.00	87.40	110.0	78.10
7	1.22	-690.0	18.00	88.40	110.0	79.10

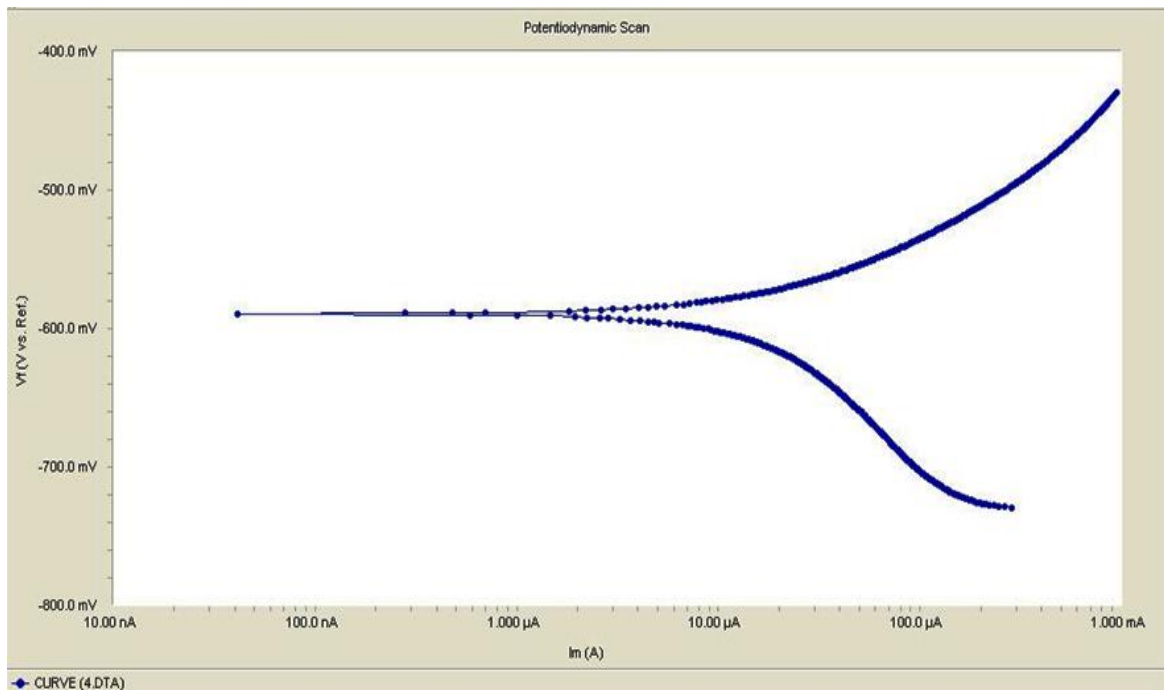


**Fig. 5.4: Corrosion potential ( $E_{\text{corr}}$ ) and Corrosion current ( $I_{\text{corr}}$ ) for base metal**

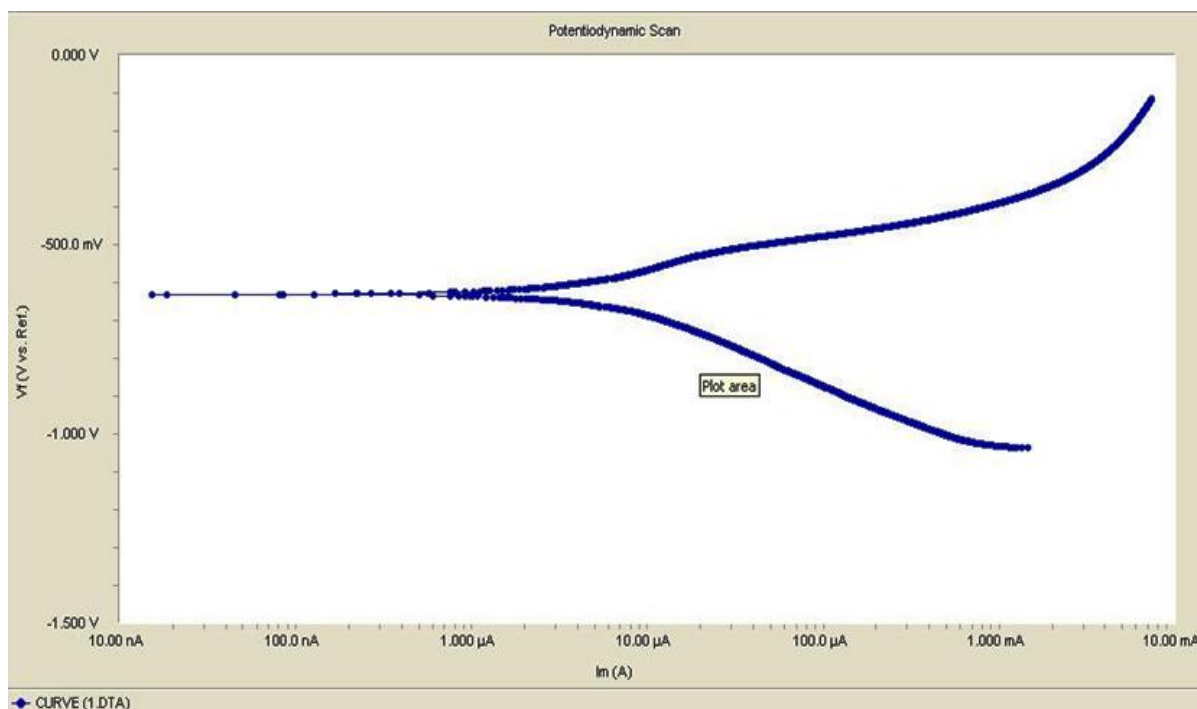


**Fig.5.5: Corrosion potential ( $E_{\text{corr}}$ ) and Corrosion current ( $I_{\text{corr}}$ ) for flux 1**

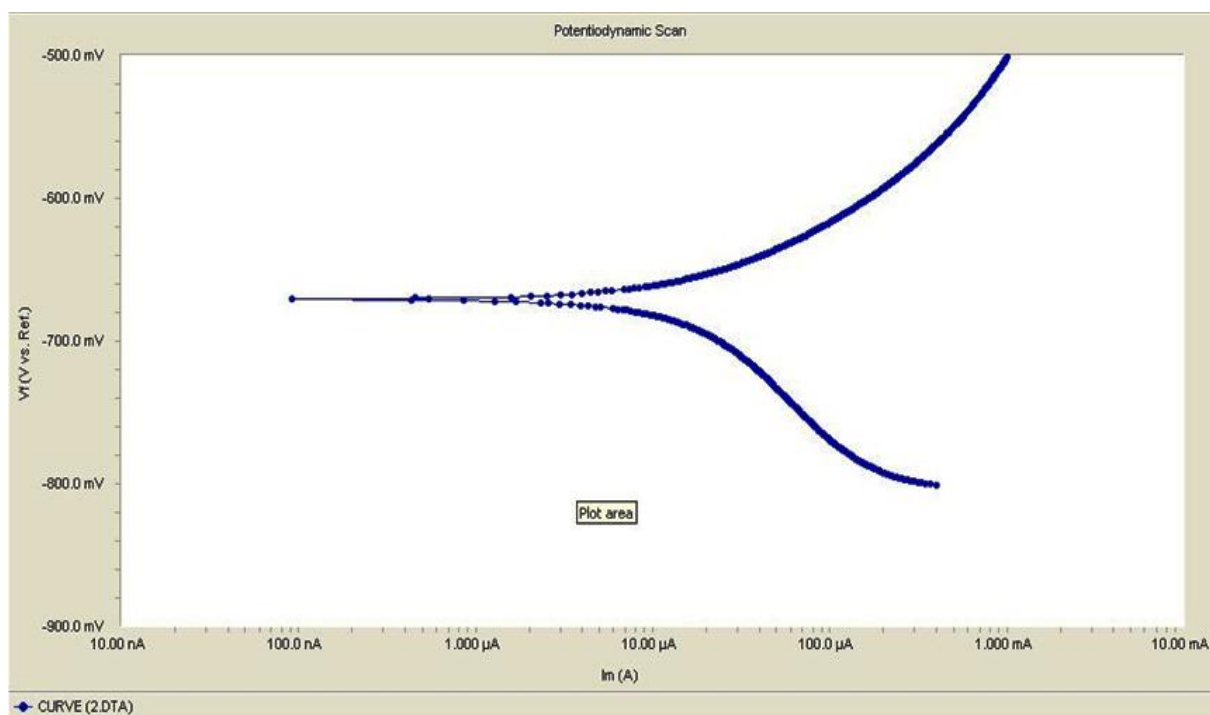


**Fig.5.6: Corrosion potential ( $E_{\text{corr}}$ ) and Corrosion current ( $I_{\text{corr}}$ ) for flux 2**

**Fig.5.7: Corrosion potential ( $E_{\text{corr}}$ ) and Corrosion current ( $I_{\text{corr}}$ ) for flux 3**

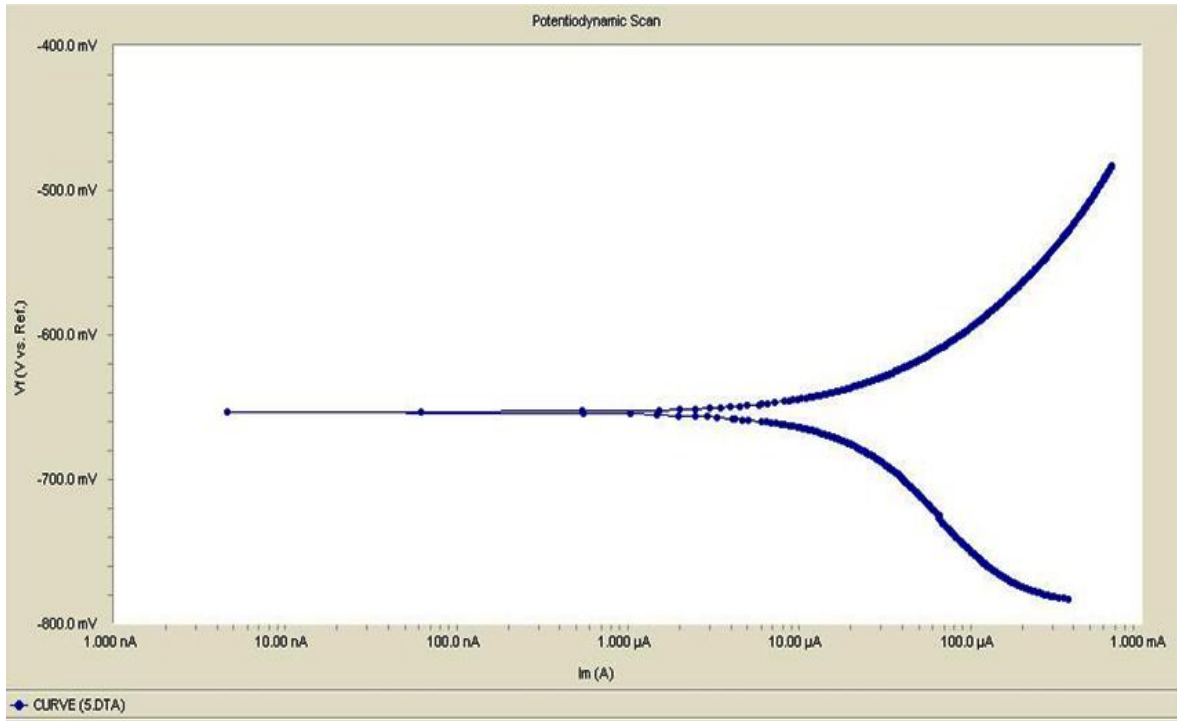


**Fig.5.8: Corrosion potential ( $E_{\text{corr}}$ ) and Corrosion current ( $I_{\text{corr}}$ ) for flux 4**

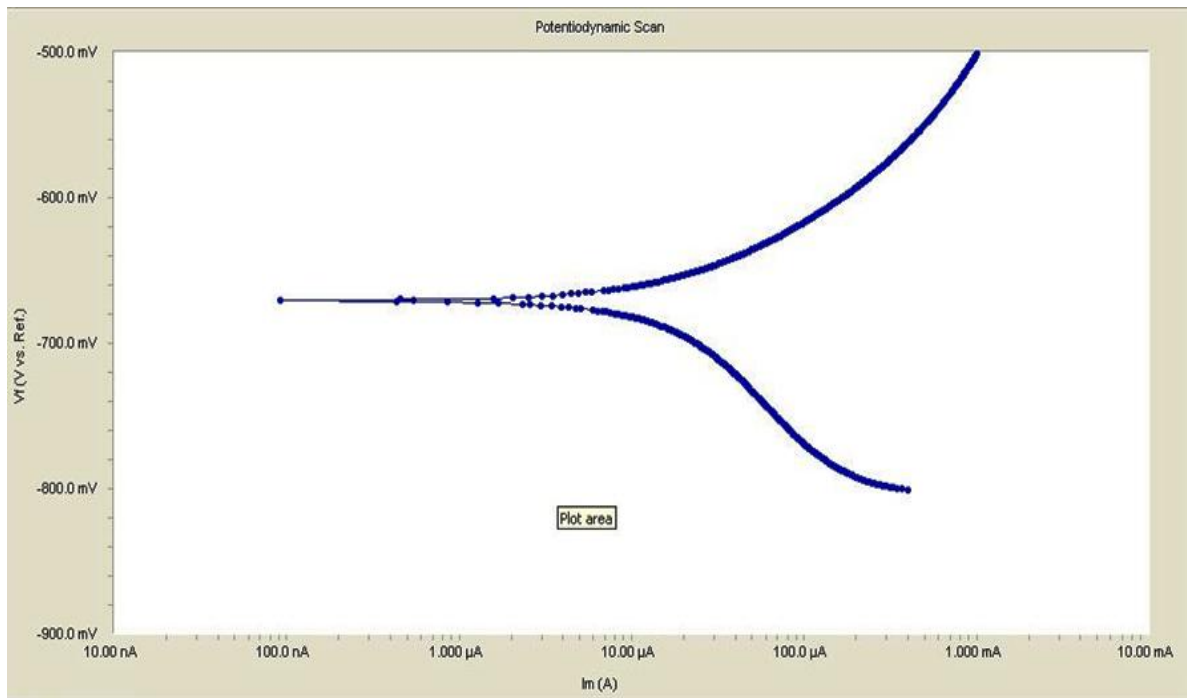


**Fig.5.9: Corrosion potential ( $E_{\text{corr}}$ ) and Corrosion current ( $I_{\text{corr}}$ ) for flux 5**

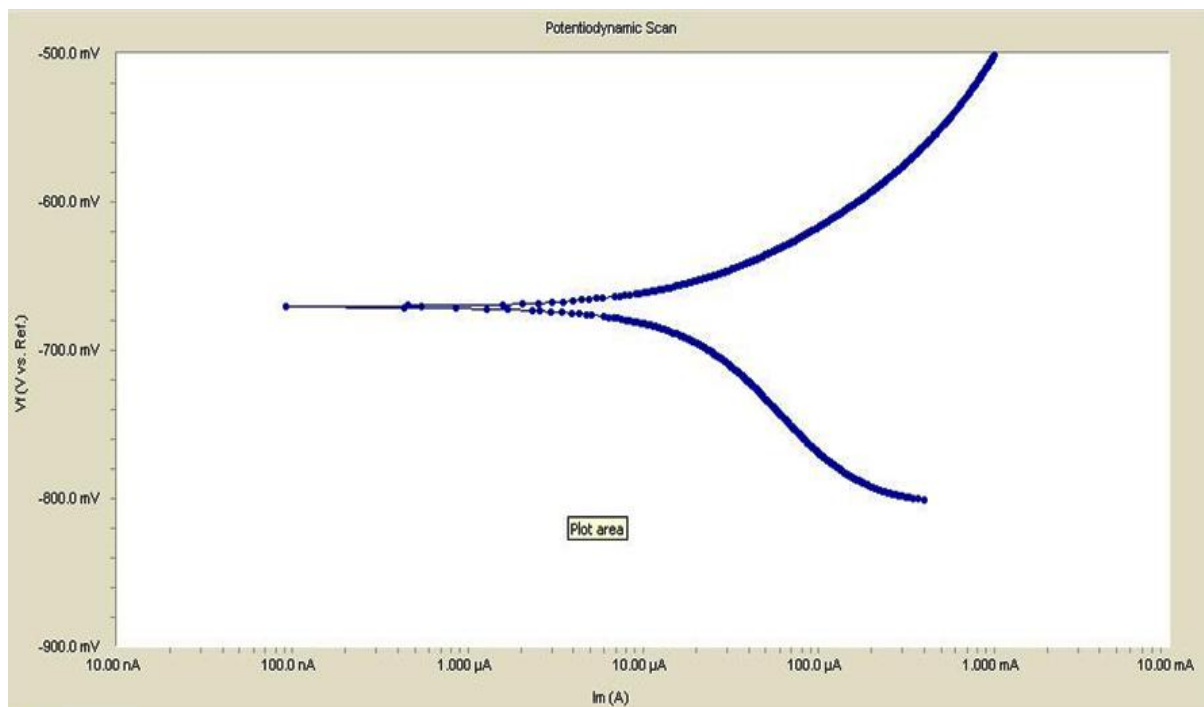


**Fig.5.10: Corrosion potential ( $E_{\text{corr}}$ ) and Corrosion current ( $I_{\text{corr}}$ ) for flux 6**

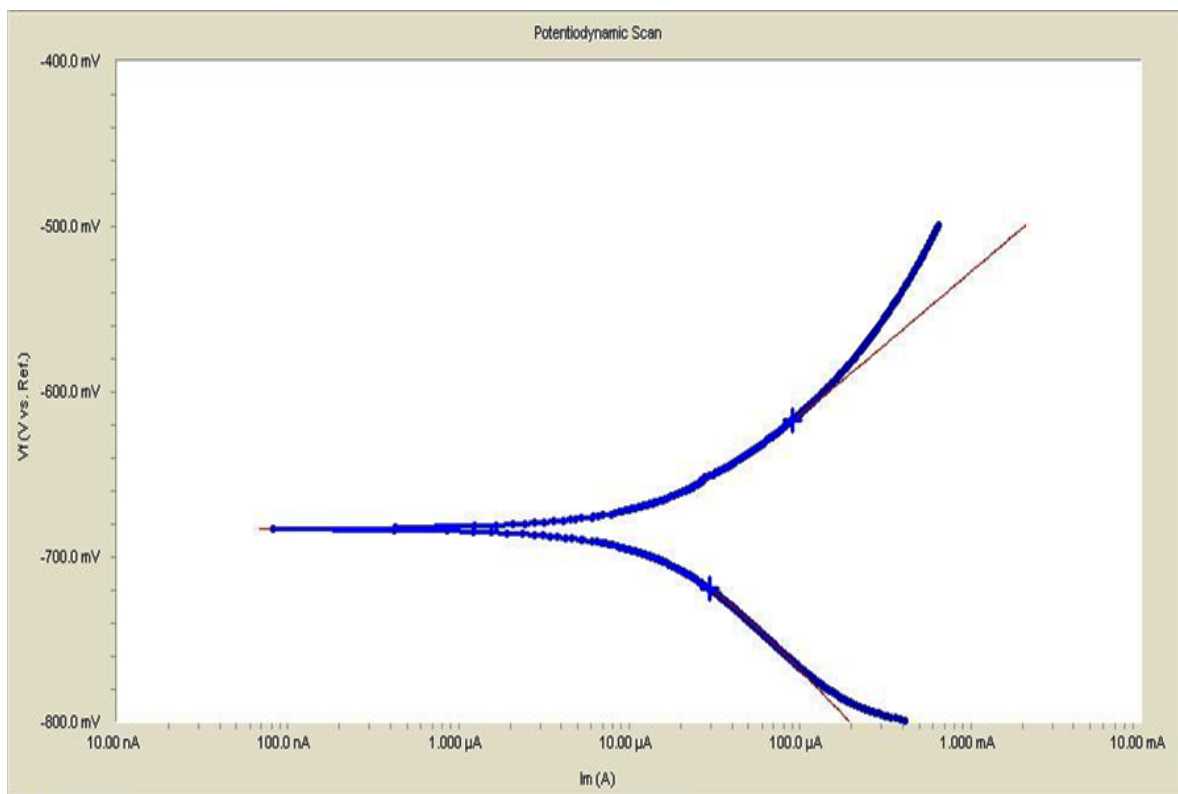


**Fig.5.11: Corrosion potential ( $E_{\text{corr}}$ ) and Corrosion current ( $I_{\text{corr}}$ ) for flux 7**

### Discussion of Corrosion Test by Polarization Scan

The polarization curve of base metal and different fluxes obtained in 0.9% NaCl solutions shown in Fig. 5.4-5.11. Potential up to  $\pm 150$  mv from open circuit potential (OCP) were made for Tafel method and a plot of E vs. log I was made in the experiment and tangents were drawn which on extrapolation to  $E_{\text{corr}}$  intersected at a point that represented on the X axis, the  $I_{\text{corr}}$  values, were obtained using the formula ( $I_{\text{corr}} = b_a b_c / (b_a + b_c) / 2.303 R_p$ ). It is clear from the table 5.2 that corrosion rate is maximum for base metal. Lesser the corrosion rate means more is the corrosion resistance and vice versa. For all the specimens corrosion rate is less than that of base metal and values obtained are nearly equal for fluxes except specimen no. 1 & 4. There is a substantial decrease in the values of corrosion rate for specimen no. 1 & 4. Generally corrosion rate depends upon the corrosion current density, higher the value of the corrosion current density ( $I_{\text{corr}}$ ), higher will be the corrosion rate and vice versa.

### 5.2 (b) Corrosion Test by Half-Cell Potential

The detection of corrosion by using the method of potential measurement is one of the most common procedures for the routine inspection of metals or alloys. The half-cell potential is measure of electrode potential, represents the potential difference between the metal and the adjacent electrolyte. Table 5.3 shows the standard values for Half Potential Cell.

**Table 5.3: Standard values of Half Cell Potential**

S.No.	Standard Potential Value	Corrosion Percentage
1	If potential is more +ve then -200 mv	90% no corrosion
2	-200 m v to -350 mv	Uncertain corrosion (may or may not be)
3	More -ve than 350 mv	90% Corrosion

**Table 5.4: Corrosion Testing of Specimen**

S. no	Flux	Corrosion Potential Value	%age Change
1	Base metal	-650.18 m v	
2	1	-590.39 m v	190.76
3	2	-553.88 m v	185.07
4	3	-600.22 m v	192.23
5	4	-556.11 m v	185.54
6	5	-547.67 m v	184.11

7	6	-560.83 m v	186.15
8	7	-602.19 m v	192.61

According to the standard values as shown in Table 5.3, if standard potential value is more negative than -350 mv (-351, -352, -353, -354.....) means metal is more prone to corrosion and 90% chances are there for the corrosion to occur. In Fig.5.12, corrosion potential values are more negative than -350mv, which ensures the occurrence of corrosion. All the values are nearly equal but slightly less than that of base metal.

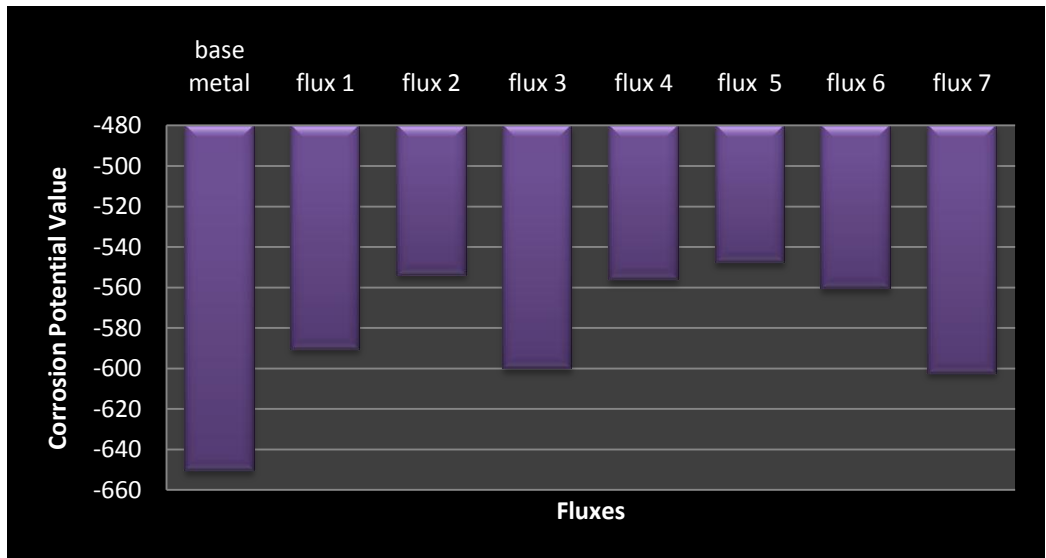


**Fig. 5.12: Corrosion test by Half-Cell Potential**

**5.2 (c) Corrosion Test by Weight Loss:**

All the specimens were first weighed before dipping in water bath and then again weighed after seven days to calculate the weight loss.



**Fig. 5.13: Specimens in water bowl**



**Fig. 5.14: Specimens in water bowl with scale**

Fig. 5.13 shows the specimens dipped in water bowl and formation of scale on specimens after seven days Fig. 5.14.

**Table 5.5: Weight loss**

S.No	B.I	Initial Wt. of Specimens (gm)	Weight After Seven Days (gm)							Avg. Wt. (gm)	% Change In Weight (gm)
			1	2	3	4	5	6	7		
Base metal		35.90	35.99	35.99	35.88	35.77	35.87	35.65	35.55	35.77	0.36
1	1.87	29.90	29.98	29.78	29.99	29.87	29.96	29.69	29.79	29.79	0.37
2	1.16	30.42	30.41	30.52	30.66	30.58	30.78	30.83	30.88	30.67	-0.88
3	1.02	30.51	30.45	30.56	30.72	30.98	30.67	30.86	30.54	30.66	-0.49
4	1.54	35.70	35.10	35.53	35.67	35.49	35.68	35.59	35.58	35.58	0.33
5	1.96	34.0	34.10	34.23	34.29	34.38	34.19	34.16	34.18	34.18	-0.52
6	1.32	33.60	33.56	33.85	33.63	33.92	33.28	33.49	33.59	33.57	0.08
7	1.22	33.40	33.43	33.36	33.58	33.49	33.29	33.19	33.48	33.48	-0.23

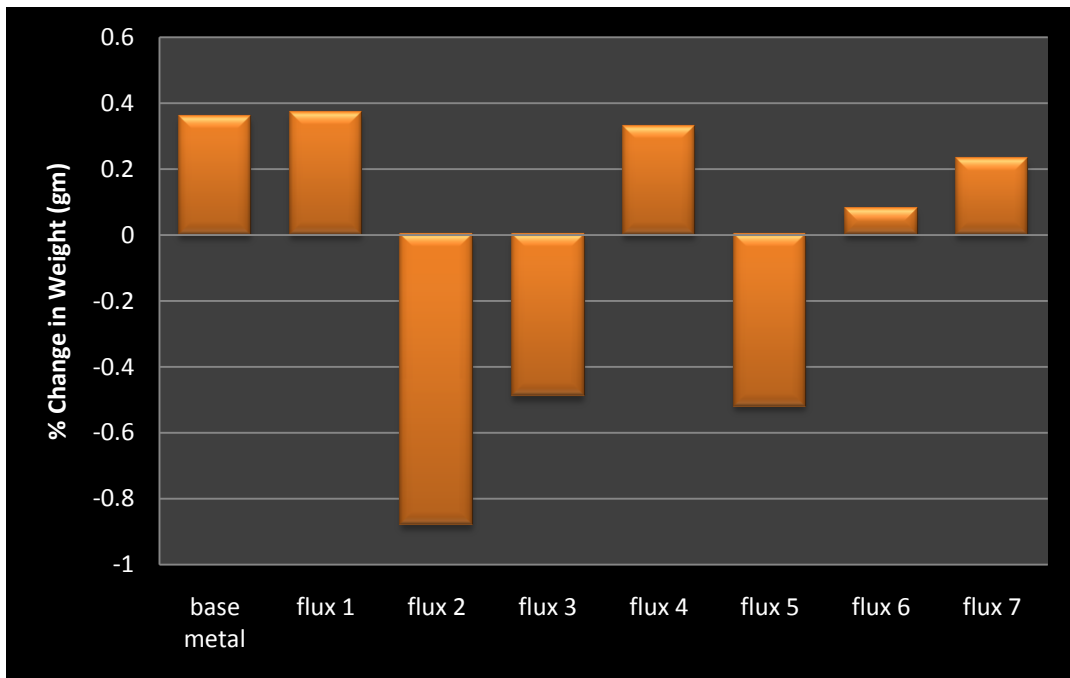


**Fig. 5.15: %age change in weight**

### Discussion of Corrosion Test

Table 5.5 shows the weight loss values of specimens and percentage change with respect to initial value taken before testing. Some of the constituents of metals are dissolved in water which results in weight loss of the specimens shown by the positive values in Fig. 5.15. In Fig. 5.4 scale formations occurs on the whole surface of the specimen which results in wt. gain shown by the negative values in Fig. 5.15.

### 5.3 MICROSTRUCTURE EXAMINATION

The following are the micrographs captured on optical microscope for microstructure examination:

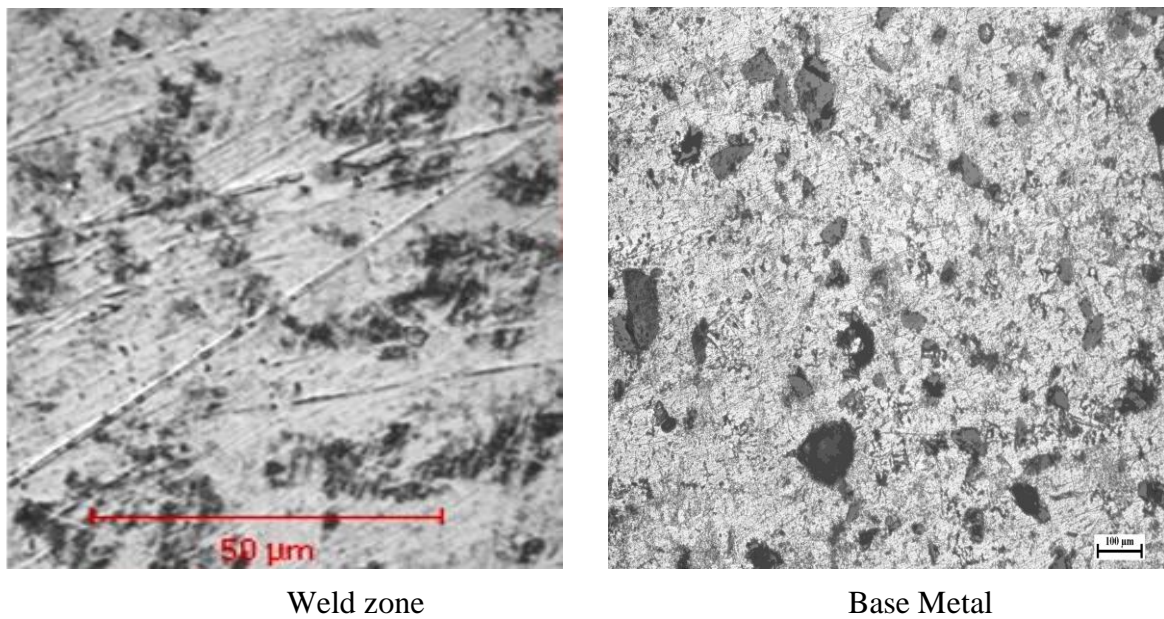
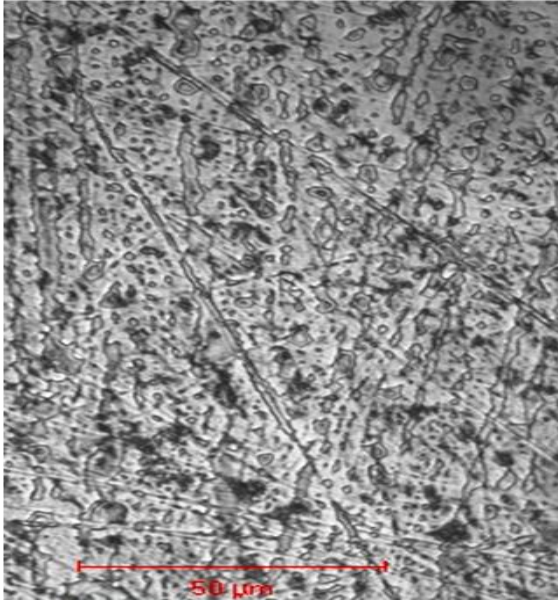
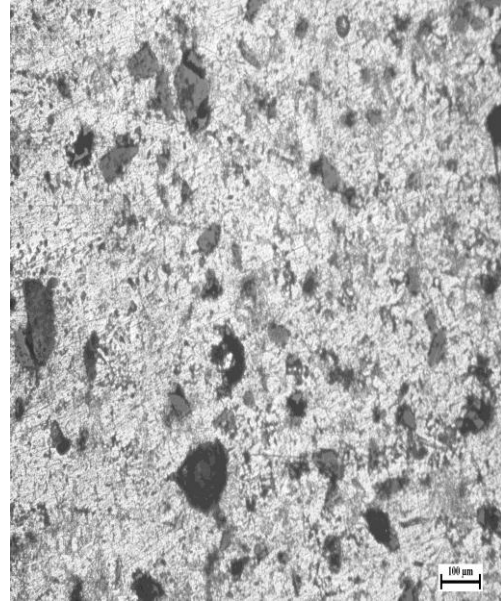


**Fig. 5.16: Microstructure of flux 1 at x500 magnificationA**

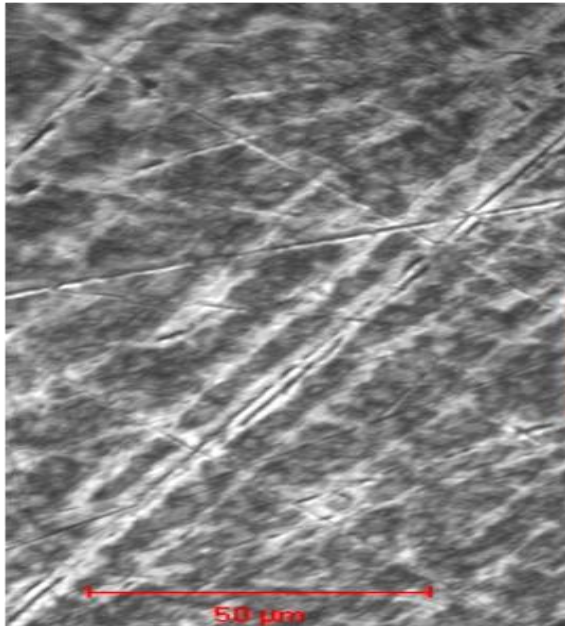


Weld zone

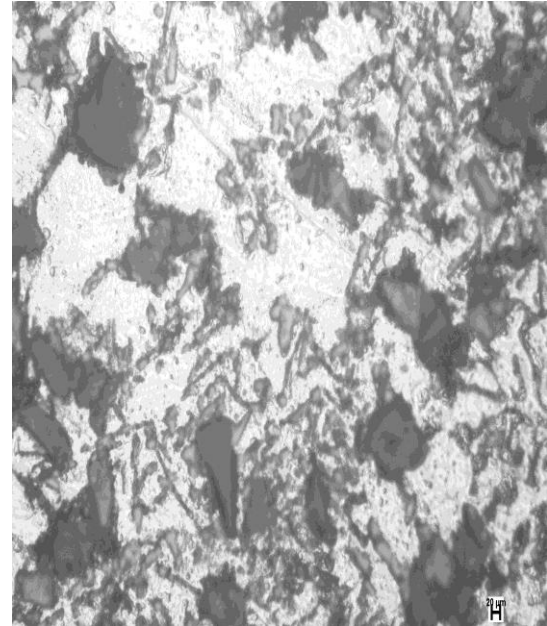


Base Metal

**Fig. 5.17: Microstructure of flux 2 at x500 magnification**



Weld zone

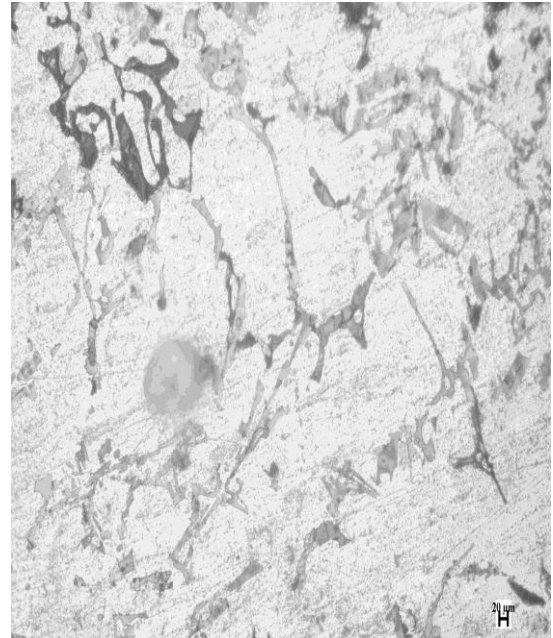


Base Metal

**Fig. 5.18: Microstructure of flux 3 at x500 magnification**

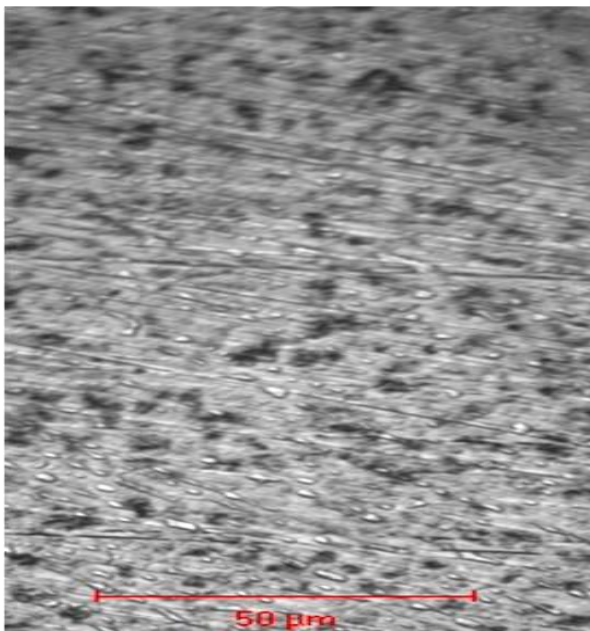


Weld zone

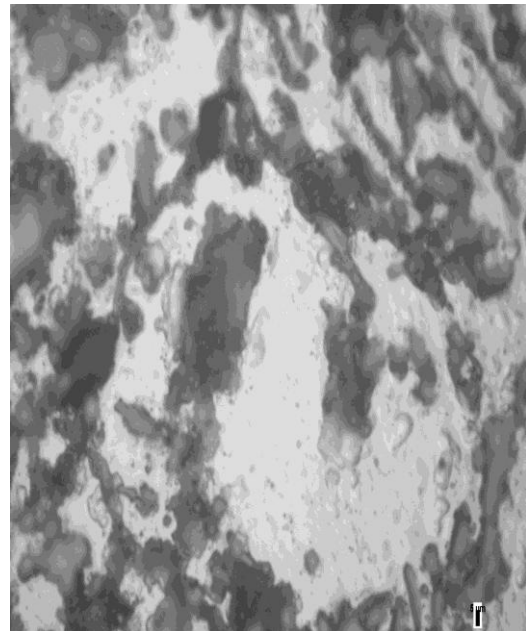


Base Metal

**Fig. 5.19: Microstructure of flux 4 at x500 magnification**

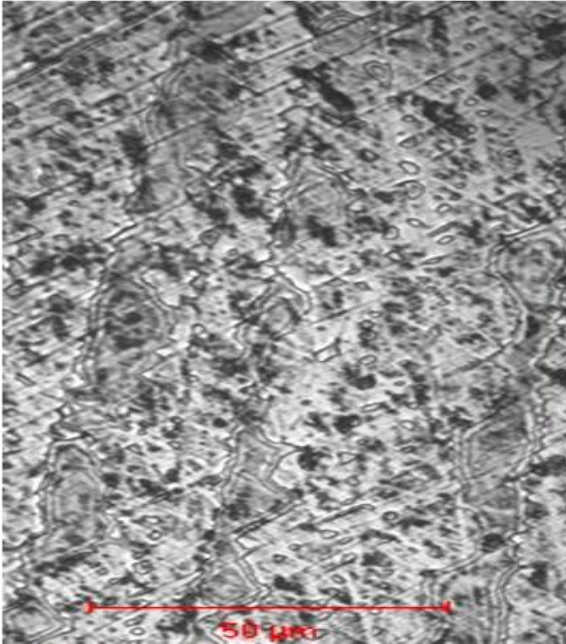


Weld zone

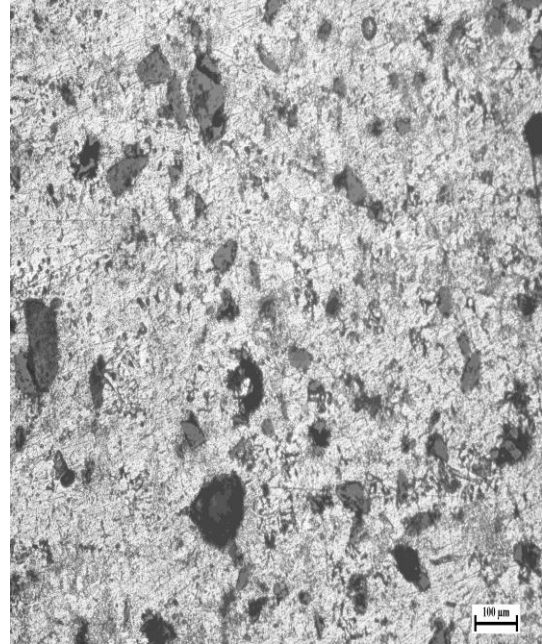


Base Metal

**Fig. 5.20: Microstructure of flux 5 at x500 magnification**

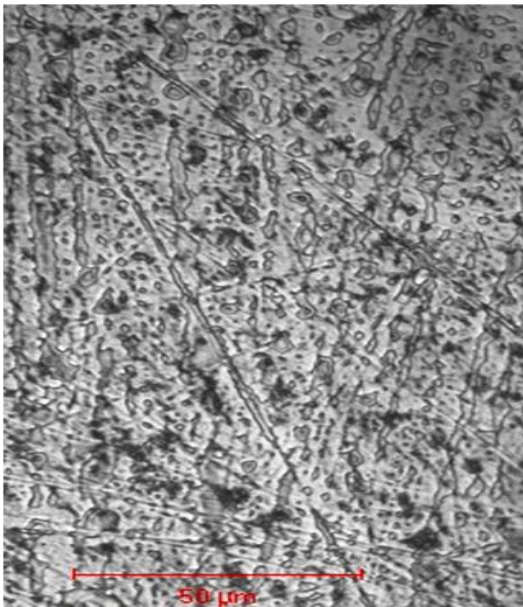


Weld zone

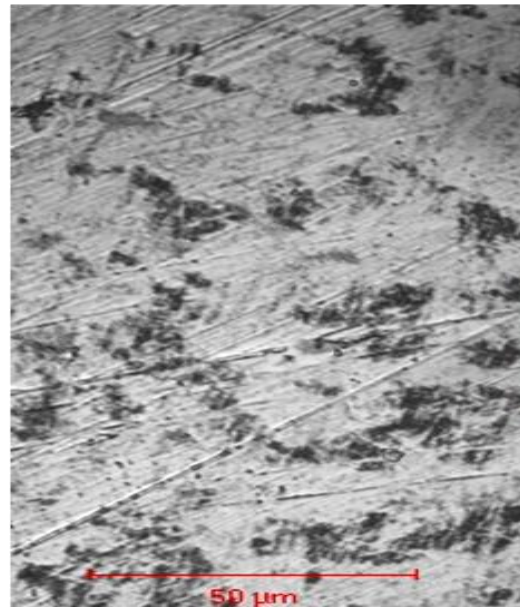


Base metal

**Fig. 5.21: Microstructure of flux 6 at x500 magnification**



Weld Zone



Base metal

**Fig. 5.22: Microstructure of flux 7 at x500 magnification**

### Discussion of Microstructure

The microstructure of Plain Carbon steel at magnifications of x500 is shown in Figures 5.16-5.22. The micrograph of the figures reveals the presence of typical dendritic (bright)-pearlite (dark) microstructure. SAW involves many metallurgical phenomena, such as melting, freezing, solid state transformations, thermal strains and shrinkage stresses. The metallurgy of SAW is complex and depends on the compositions of the parent metal, the filler rod, and the flux, as well as on the welding parameters such as polarity, heat input, number of passes, etc. Although the composition of the filler rod is generally similar to that of the parent metal, the weld metallurgy is Complicated because the weld metal composition comes from the filler rod, parent metal and micro elements of the flux. At the same time, the different temperatures to which different weld zones are subjected result in a heterogeneous cooling rate in the weld joint. Thus, the microstructures of a weld joint are different from zone to zone. The microstructure of the weld metal is mainly coarse columnar grains, due to the relatively high heat input, large weld pool and fast solidification. Low toughness and hydrogen cracking of the weld metal results from the columnar microstructure in the weld metal.

### 5.4 MICROHARDNESS TEST

Micro hardness values at welded region for different types of fluxes are shown in table 5.6. Micro hardness test was performed at a constant load of 300 gm. For each specimen two readings were taken and the average of these two readings was calculated. Fig. 5.23-5.30 shows the indent on welded region.

**Table 5.6: Micro hardness values at welded region**

S. No	Flux	Basicity Index	Indentation Load(gm)	Hardness value(HV)	Hardness value(HV)	Average Hardness(HV)
Base Metal			300	222 HV	188 HV	205
1	1	1.87	300	219 HV	224 HV	221.5
2	2	1.16	300	293 HV	278 HV	288
3	3	1.02	300	259HV	251 HV	255
4	4	1.54	300	219HV	217 HV	218
5	5	1.96	300	227 HV	190 HV	208.5
6	6	1.32	300	241 HV	234HV	237.5
7	7	1.22	300	173 HV	169HV	171

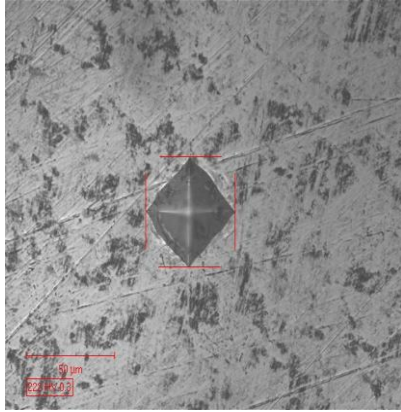


**Fig. 5.23: Micro hardness of Base metal**

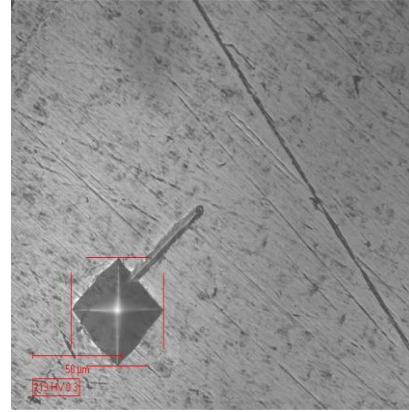


**Fig. 5.24: Micro hardness of flux 1**

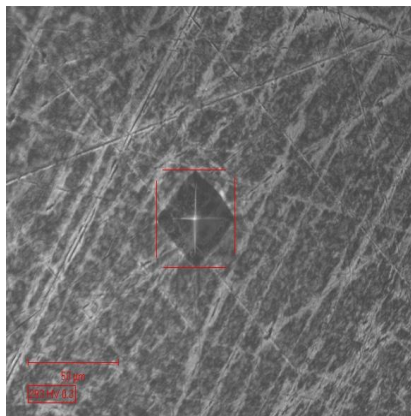


**Fig. 5.25: Micro hardness of flux 2**

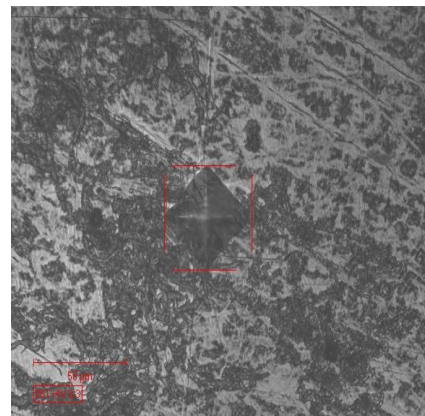


**Fig 5.26: Micro hardness of flux 3**

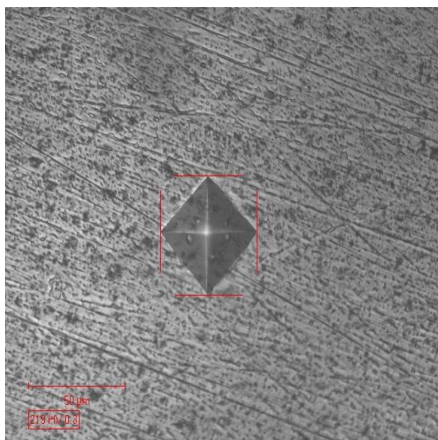


**Fig 5.27: Micro hardness of flux 4**

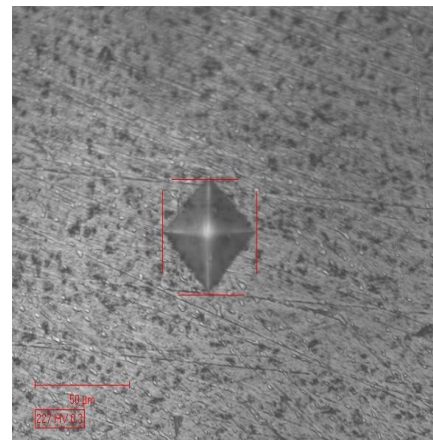


**Fig .5.28: Micro hardness of flux 5**

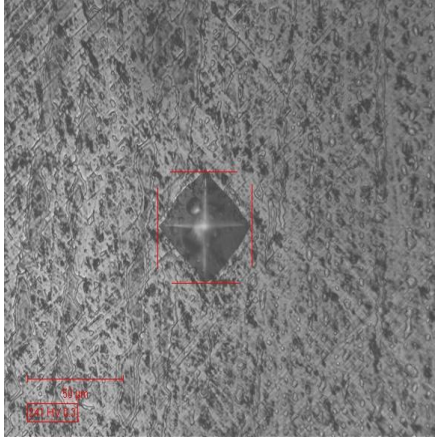


**Fig.5.29: Micro hardness of flux 6**

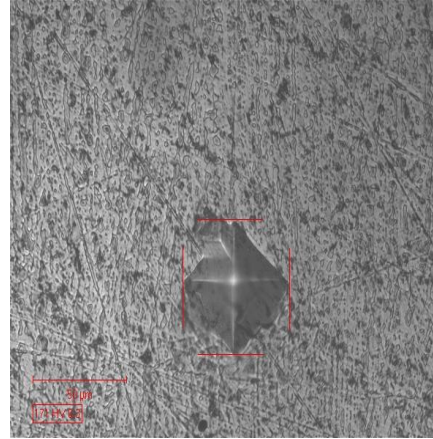


**Fig. 5.30: Micro hardness of flux 7**

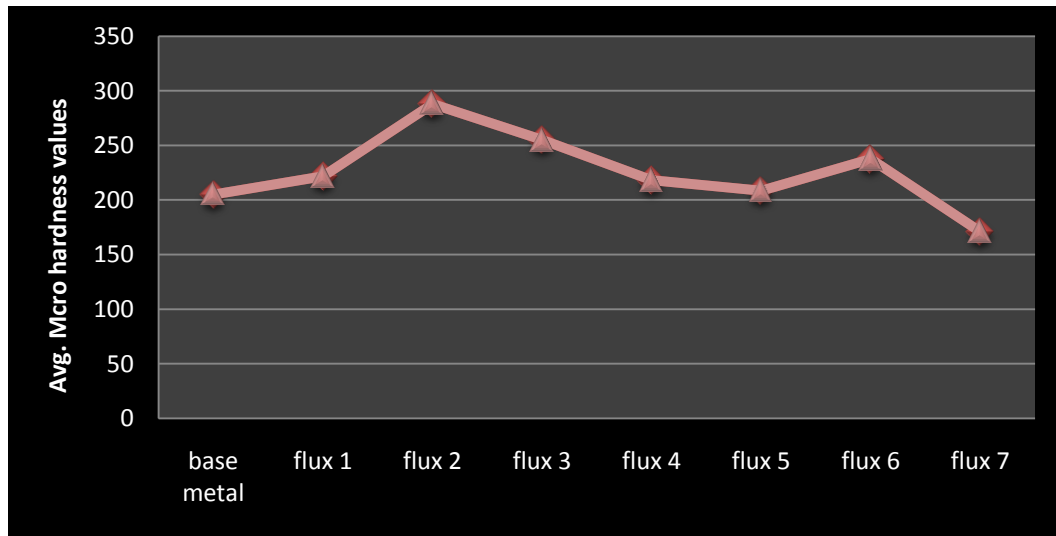


**Fig.5.31: Micro hardness with different fluxes**

### **Discussion of Micro hardness**

Microhardness measurement was taken at the base metal and weld pool interface. Two readings at each location were taken & average of two readings was considered for the analysis. It is clear from fig 5.23 that the max. average micro hardness (Vickers hardness number) was observed at welded region for flux 2, this is due to the presence of carbides constituents present in the flux, hardness value in the weld metal changes with the change in the carbide contents. The increase in microhardness at the welding interface is generally due to oxidation processes which took place during welding processes.

## 5.5 TENSILE TEST

Universal tensile testing machine was used to carry out tensile tests. Fig. 5.24 below shows the broken specimen after tensile test.



**Fig. 5.32: Specimen after tensile test**

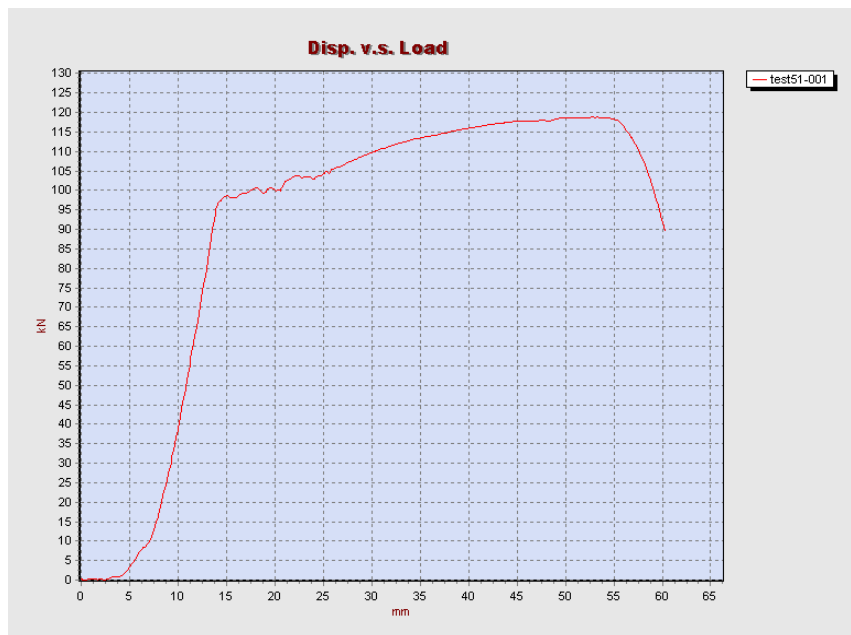


**Fig. 5.33: Load vs. displacement curve for base metal**

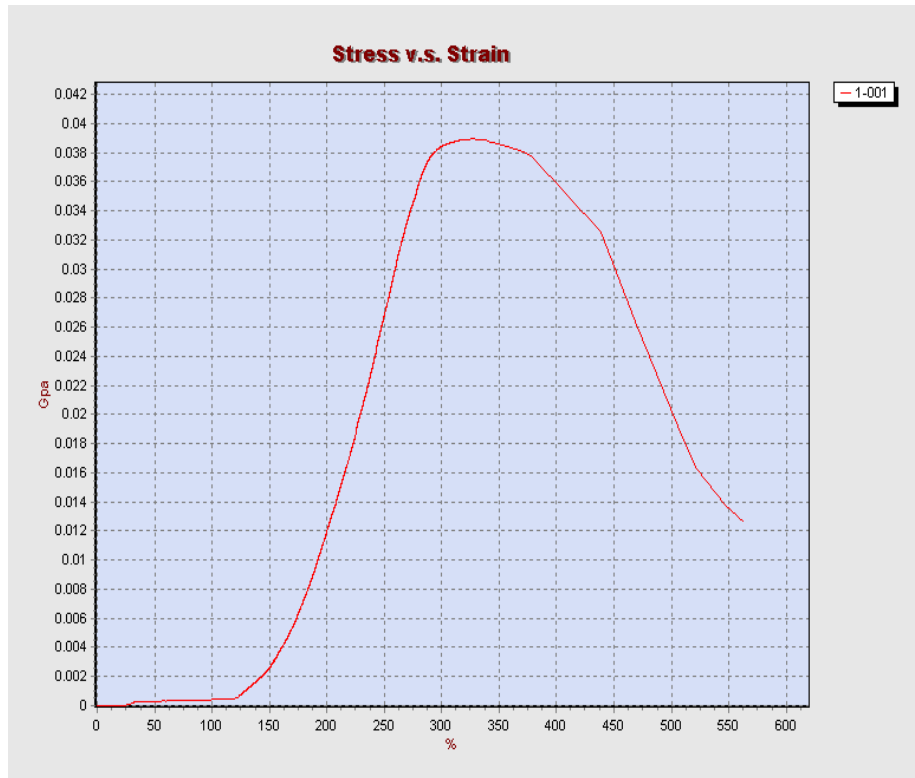


**Fig. 5.34: stress vs. strain curve for base metal**

**Table 5.7: Ultimate Tensile Strength Readings**

Flux	Basicity Index	Ultimate Tensile Strength (KN)
Base Metal		95.12
1	1.87	44.50
2	1.16	35.60
3	1.02	47.90
4	1.54	43.40
5	1.96	26.60
6	1.32	29.40
7	1.22	31.10

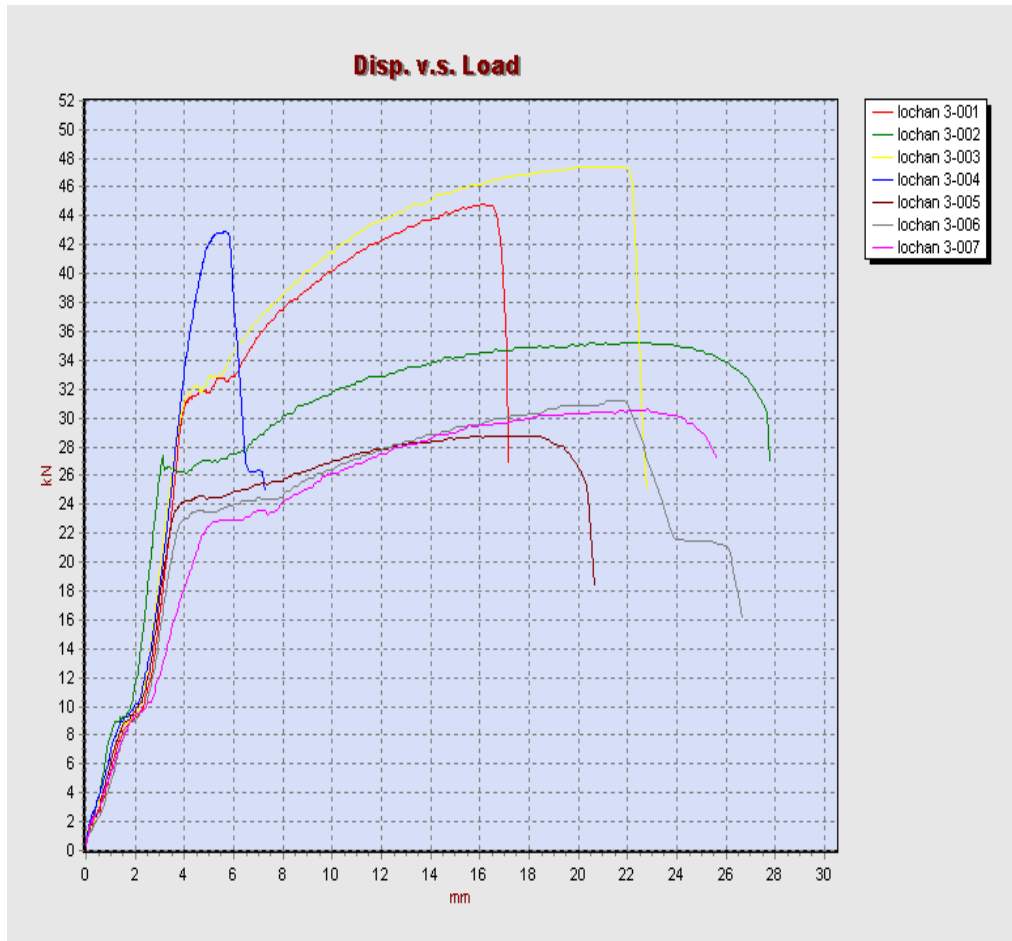


**Fig. 5.35: Load vs. displacement curve for 7 different welded specimens**

**Table 5.8: Ultimate Tensile Stress Readings**

Flux No.	Basicity Index	Tensile Stress Values (Gpa)
Base Metal		0.038
1	1.87	0.058
2	1.16	0.045
3	1.02	0.056
4	1.54	0.053
5	1.96	0.034
6	1.32	0.038
7	1.22	0.036

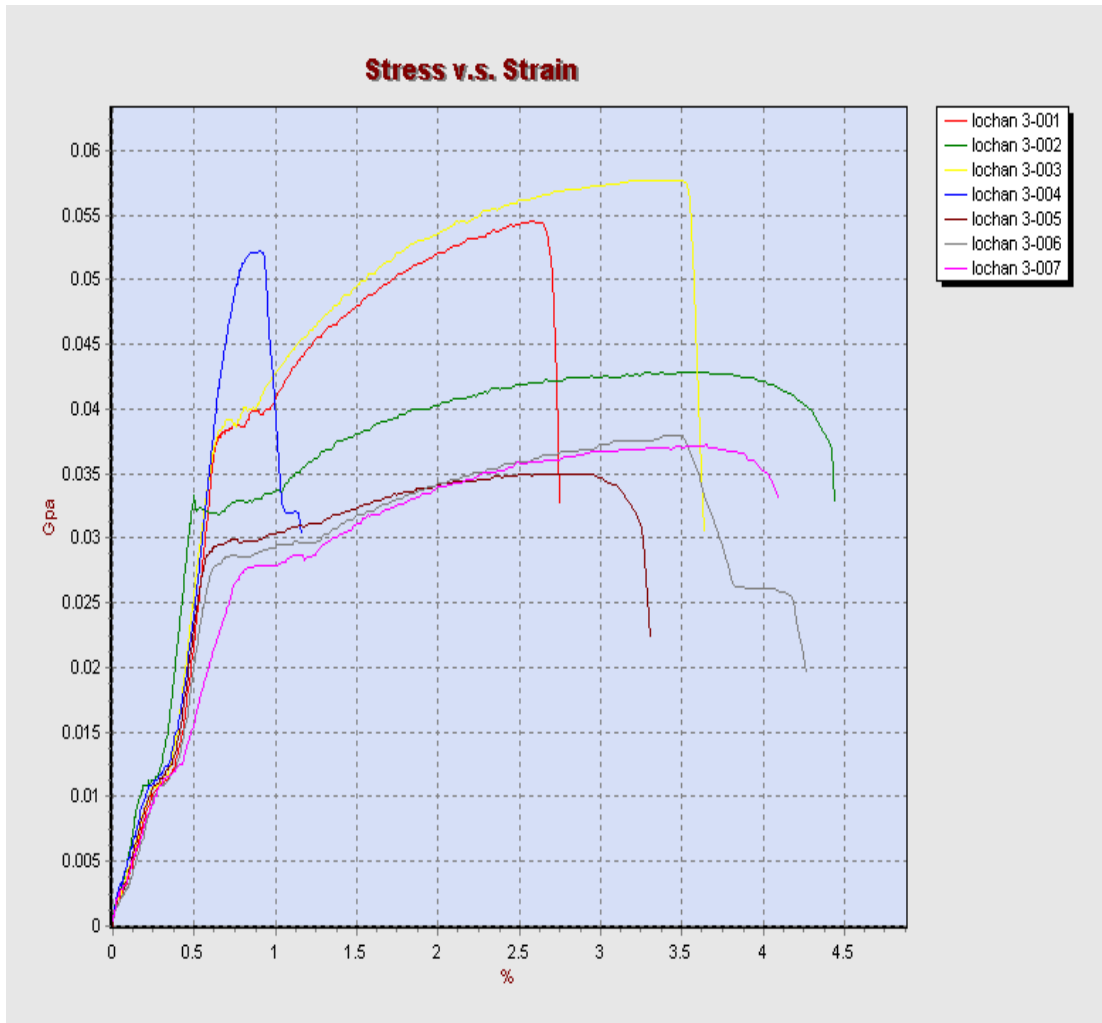


**Fig. 5.36: Stress vs. Strain curve for 7 different welded specimens**

**Discussion of tensile test**

Submerged Arc Welding is a fusion welding process in which heat is produced from an arc between the work and a continuously fed filler metal electrode. During welding process there change in mechanical properties due to change in elemental components of parent metal and the filler electrode which cause microstructural changes, from the base material. The effect of various fluxes on Ultimate Tensile Strength and Ultimate Tensile Stress of the welded joints were examined. From table 5.7-5.8 and fig.5.35-5.36, it appears that maximum ultimate tensile strength was observed for specimen no 3 i.e. 47.90 KN and for specimen no. 1 and 4 values obtained were nearly equal to specimen no. 3. The lowest ultimate tensile strength for specimen no. 5 was obtained and for specimen no. 2, 6 and 7 values are nearly

equal to specimen no 5 i.e. 26.60 KN. It is clear from the table 5.7 that with the increase in basicity index tensile strength observed was minimum and vice versa.

## 5.6 CHEMICAL COMPOSITION OF WELD METAL

The specimens after composition at welded region is shown in fig 5.40



**Fig 5.37: Specimen after checking composition**

**Table 5.9 Percentage Change and Change in Percentage Composition of Carbon and Manganese**

Flux	Carbon	Carbon in electrode	% change in Carbon	Manganese	Manganese in electrode	% change in Manganese
Base metal	0.221	0.05	342	0.490	0.1	390
1	0.143	0.05	182	0.601	0.1	501
2	0.125	0.05	150	1.350	0.1	1250
3	0.188	0.05	276	0.549	0.1	449
4	0.883	0.05	1666	1.27	0.1	1170
5	0.203	0.05	306	0.471	0.1	371
6	0.105	0.05	110	0.861	0.1	761

7	0.045	0.05	-10	0.901	0.1	780
---	-------	------	-----	-------	-----	-----

**Table 5.10 Percentage Change and Change in Percentage Composition of Silicon and Chromium**

Flux	Silicon	Silicon in Electrode	% change in Silicon	Chromium	Chromium in electrode	% change in Chromium
Base metal	0.209	0.1	109	0.055	0.0	5.5
Flux 1	0.402	0.1	302	0.070	0.0	7
Flux 2	0.403	0.1	303	0.030	0.0	3
Flux 3	0.230	0.1	130	0.119	0.0	11.9
Flux 4	0.210	0.1	110	0.032	0.0	3.2
Flux 5	0.197	0.1	97	0.167	0.0	16.7
Flux 6	0.227	0.1	127	0.050	0.0	5
Flux 7	0.289	0.1	189	0.037	0.0	3.7

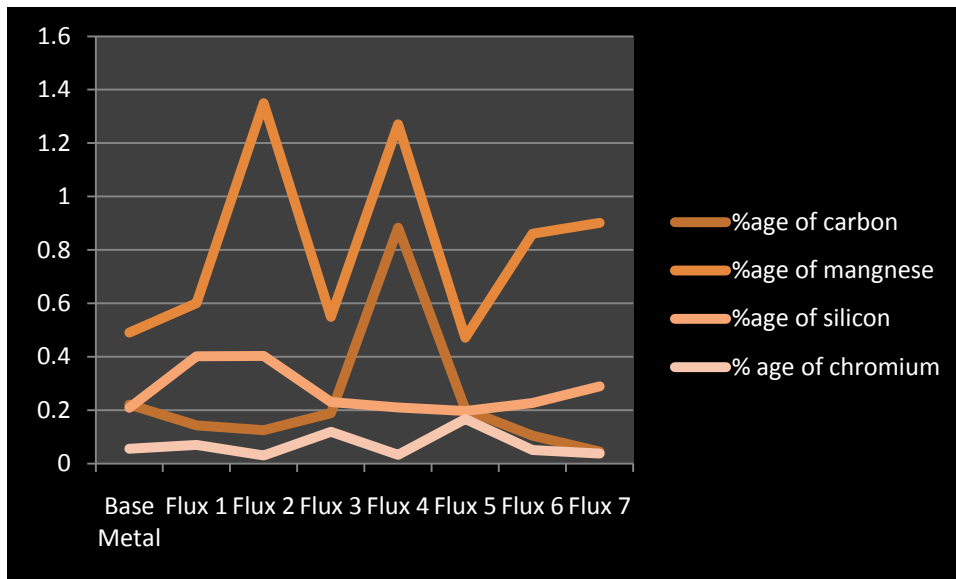


**Fig. 5.38: Percentage Composition of C, Mn, Si and Cr in weld metal**

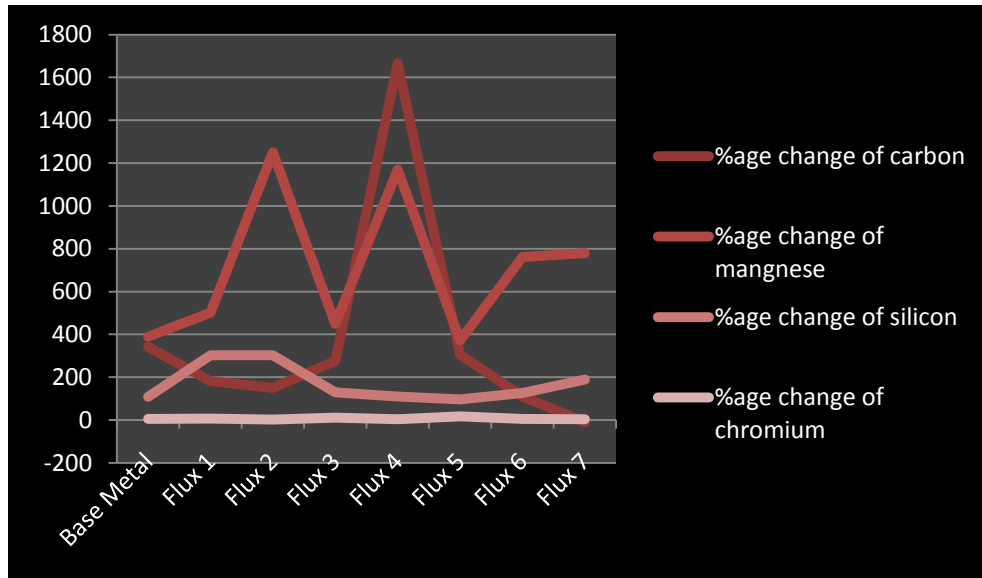


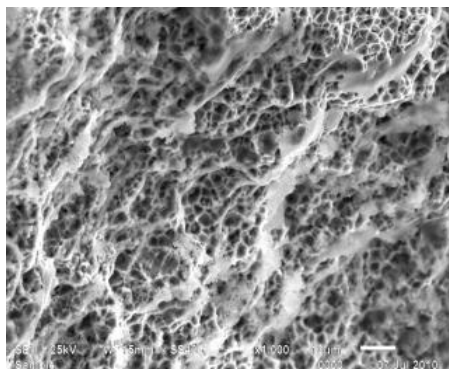
**Fig. 5.39: Percentage Change in Composition of C, Mn, Si and Cr in weld metal**

### Discussion of Chemical composition

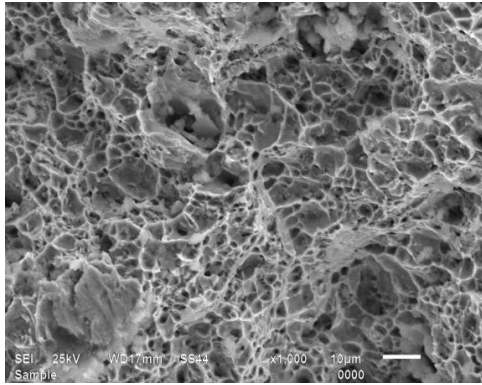
Chemical composition values are listed in table 5.9 and 5.10. There is sudden increase and decrease in percentage of manganese. There is substantial change in carbon for flux 4. Percentage changes occur due to the elemental diffusion from flux towards base metal. The amount of transfer is however different depending on the flux composition. More basic flux yield less negative carbon and manganese though the reduction of oxygen content in the weld metal.

## 5.7 SCANNING ELECTRON MICROSCOPE (SEM)

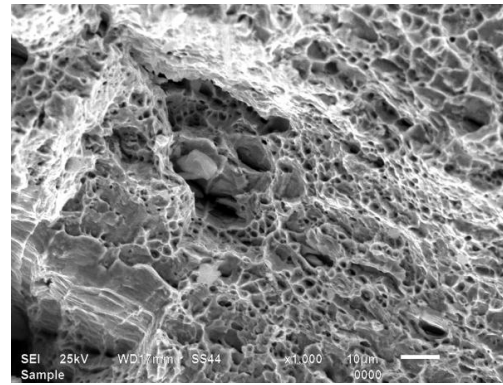
Scanning electron microscope (SEM) of different tensile test specimens shown in fig:



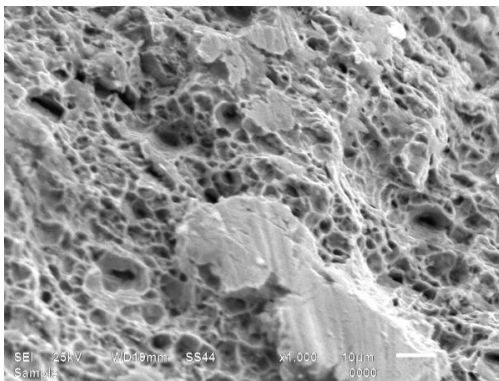
Base Metal



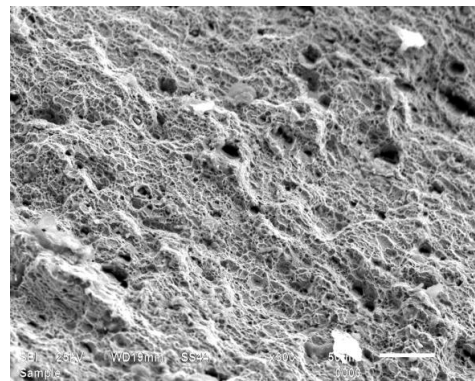
(1)



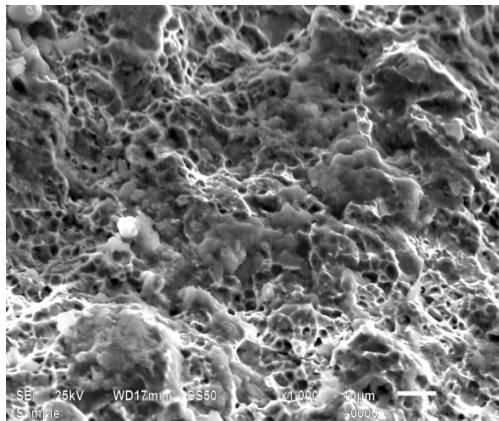
(2)



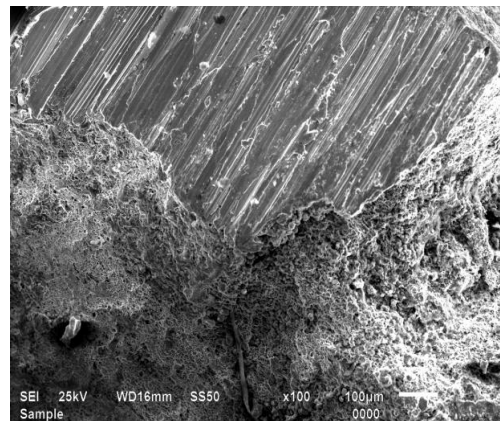
(3)



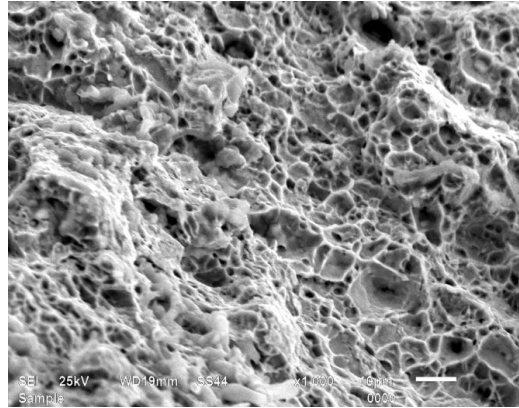
(4)



(5)

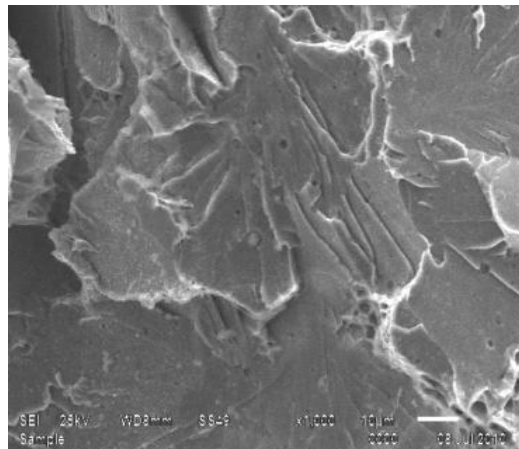


(6)

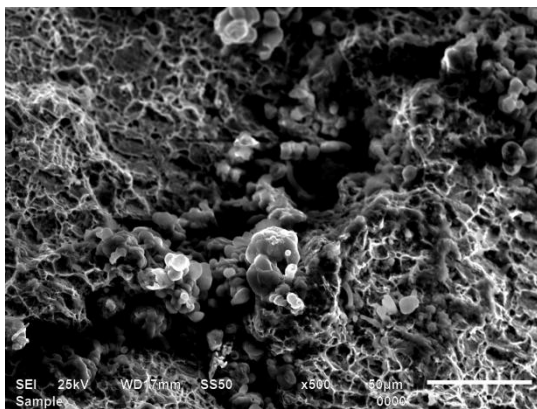


(7)

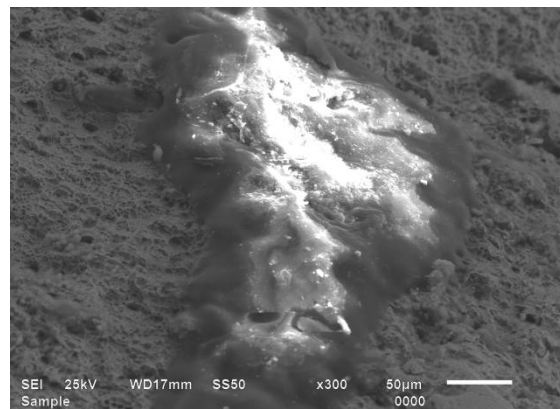
**Fig 5.40: SEM measurement at x1000 magnification for specimen after breakage of tensile test which weld from by using welding flux (1), (2), (3), (4), (5), (6), (7)**



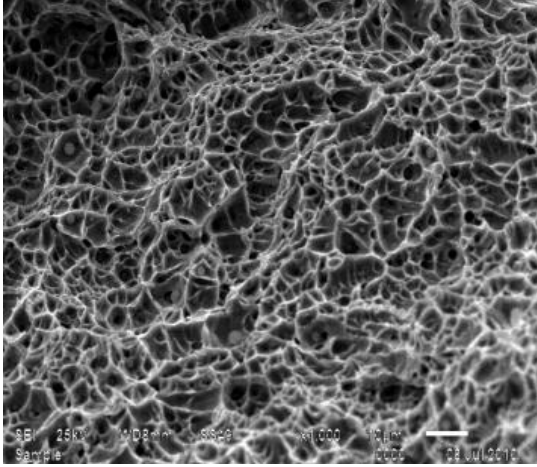
**Base Metal**



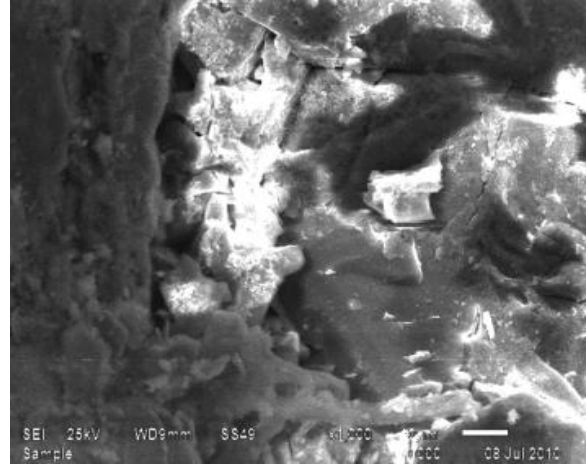
(1)



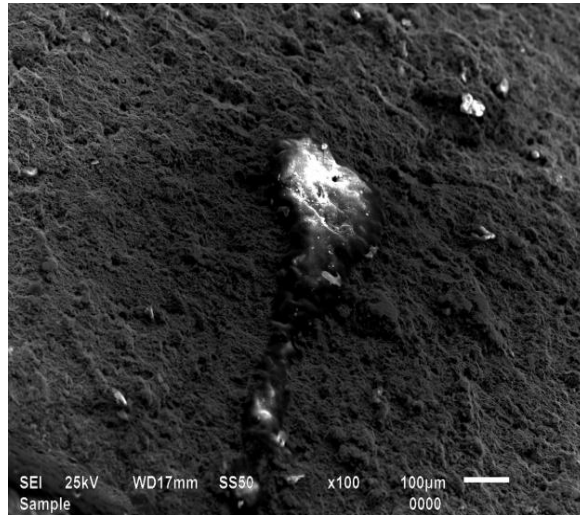
(2)



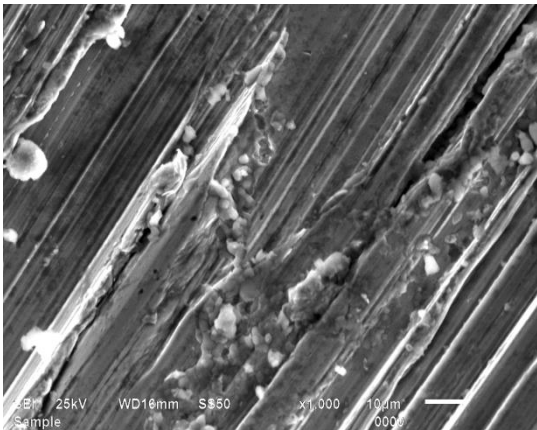
(3)



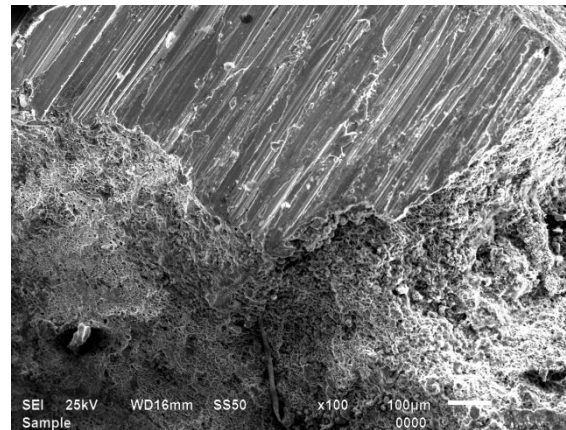
(4)



(5)



(6)



(7)

**Fig 5.41: SEM measurement at x1000 magnification for specimen after breakage of toughness at room temperature which weld from welding flux (1-7)**

#### **Discussion of Microstructure**

Typical SEM Fractographs of impact and tensile fracture specimens have been taken. Fig 5.40 and 5.41 shows the fractography of the base metal and fractured surface. Fractographs shows plastic deformation on the fractured surface and crack is propagated both by transgranular and intergranular manner. Fig. 5.41 (3) shows the dimples results in ductile fracture and rest of the figures shows transgranular fracture.

The present study was carried out to study the effect of fluxes on the corrosion resistance of the submerged arc welding steel welds by keeping all other variable keeping constant like current, voltage and welding speed.

- 1) Corrosion rate values for different fluxes of submerged arc steel welds were satisfactory and increase in corrosion resistance can be observed in all the specimens as compared to base metal.
- 2) The impact toughness values at room temperature increases with increase in basicity index of flux.
- 3) Oxidizing potential of the most reactive fluxes reduced by a significant amount due to the addition of  $\text{CaF}_2$ , while  $\text{CaF}_2$  has little effect on the more stable oxide components.
- 4) Ultimate tensile strength values are dependent on the basicity index. It can be concluded that more is the basicity index lesser will be the ultimate tensile strength.
- 5) Ultimate tensile strength values were also satisfactory for all weld joints.
- 6) Microstructure evaluation of the welded joints revealed Dendritic structure while base metal cleavage structure obtained.
- 7) Change in micro hardness values can be observed due to the presence of carbides.
- 8) Dimples can be seen in SEM fractographs which results in ductile fracture and transgranular fractures can be observed.
- 9) It is concluded from the above experiments that there is increase in impact toughness values, decrease in corrosion rate values and decrease in tensile strength of base metal and different fluxes.

In addition to the present work further work can be done in following directions:

- 1) Corrosion rate of Plain Carbon steel can be controlled by using different weight percentage of NaCl solution for further enhanced corrosion resistance of steel welds.
- 2) Corrosion rate of Plain Carbon steel can be controlled by using different method such as Static Immersion Test and Dynamic Immersion test and AC Impedance spectroscopy technique.

- 3) Corrosion rate can be controlled by using different inhibitors such as thiourea and Hexamine mixture at different concentration of NaCl and HCl solutions by weight percentage.
- 4) Different fluxes can be made for different material.
- 5)  $\text{CaF}_2$  can be replaced by NaF when manufacturing of flux.
- 6) Modeling of submerged arc welding process can be carried out using Finite Element packages.
- 7) There are lot of parameters (Current, voltage, welding speed, diameter of electrode) which can be varied individually to see their individual effects and combining these parameters to see their combine effect.
- 8) Various other techniques can be used for finding the corrosion resistance rate of structural steel welds.

## REFERENCES

- 1) Dr. R. S Parmar, Welding Processes & Technology, *Advani-Oerlikon limited*. 1988
- 2) [www.wikipedia.com](http://www.wikipedia.com)
- 3) [www.google.co.in](http://www.google.co.in)
- 4) [Beginners\\_guide\\_to\\_corrosion](#)
- 5) [www.corrosion.ksc.nasa.gov](http://www.corrosion.ksc.nasa.gov)
- 6) [www.corrview.com](http://www.corrview.com)
- 7) [AVP\\_Corrosion handbook](#)
- 8) [www.deltathx.com](http://www.deltathx.com)
- 9) [Svensson L. E., Elvander Johan, Esab A B and Göteborg, Challenges for welding Consumables for the new Millennium, 1999](#)
- 10) [Plessis John Du, Control of Diffusible Weld Metal Hydrogen through Arc Chemistry modification, University of Pretoria, 2006.](#)
- 11) Mitra U., Chai C. S. and Eagar T. W., Slag Metal Reactions during Submerged Arc Welding of Steel, 1984.
- 12) Serdar Karaoglu, Abdullah Secgin, Sensitivity analysis of submerged arc welding process parameters, *journal of materials processing technology*, Pg 500–507, 2008.
- 13) Kook-soo Bang<sup>1</sup>, Chan Park, Hong-chul Jung, and Jong-bong Lee, Effects of Flux Composition on the Element Transfer and Mechanical Properties of Weld Metal in Submerged Arc Welding, Pg 471-477, 2009.

- 14) Keshav Prasad & D. K. Dwivedi, Some investigations on microstructure and mechanical properties of submerged arc welded HSLA steel joints, *Journal of Advanced Manufacturing Technology*, Pg 475-483, 2006
- 15) Rquintana, Acruz, Lperdomo, Gcastellanos, Llgarcia, Afarmoso and Acores, Study of the transfer efficiency of alloyed elements in fluxes during the submerged arc welding process, *Welding international*, Pg 958-965, 2003
- 16) P. Kanjilal, T.K. Pal, S.K. Majumdar, Combined effect of flux and welding parameters on chemical composition and mechanical properties of submerged arc weld metal, *Journal of Materials Processing Technology*, Pg 223-231, 2005
- 17) J. Tusek, M. Suban, High-productivity multiple-wire submerged-arc welding and cladding with metal-powder addition, *Journal of Materials Processing Technology*, Pg 207-213, 2003
- 18) R. S. Chandel, H. P. Seon, F. L. Cheong, Effect of metal powder addition on mechanical properties of submerged arc welds, *Journal of materials science*, Pg 1785-1786, 1998
- 19) Saurav Datta & Asish Bandyopadhyay & Pradip Kumar Pal, Modeling and optimization of features of bead geometry including percentage dilution in submerged arc welding using mixture of fresh flux and fused slag, *Journal of Advanced Manufacturing Technology*, Pg 1080-1090, 2006
- 20) Eagar, T.W,1979, Oxygen and Nitrogen Contamination during arc welding, *Proc. of Weldments: Physical Metallurgy and Failure Phenomena*; Bolton Landing, Lake George; N.Y; 1979.
- 21) Tiwari, P.H, Bailey, M.G. and Eampell, A.B.,1979, erosion corrosion of carbon steel in aqueous H<sub>2</sub>S solutions up to 120 degree Celsius and 1.6MPa Pressure, *Corrosion science*,Vol.19,pp. (583 to 585).
- 22) Behcet Gulenc, Nizamettin Kahraman, Wear behaviour of bulldozer rollers welded using a submerged arc welding process, *Materials and Design* Pg 537–542, 2003
- 23) Chai, C.S and Eagar, T.W, Slag Metal Reactions in Binary CaF<sub>2</sub> -Metal oxide Welding Fluxes,1981.
- 24) Federer, J. I., Corrosion of Fluidized-Bed Boiler Materials in Synthetic Flue Gas, ORNL/TM Distribution Category UC-95.,1983.

- 25) Matsunami, K., Kato, T., Corrosion of Carbon steel and its estimation in Aqueous solution used in Petroleum Refineries,1990, Int. J. Pres. Ves. & Piping 45(179-197).
- 26) Mitra, U. and Eagar, T.W., developed the kinetic model to describe the transfer of alloying elements between the slag and metal during flux-shielded welding,1991.
- 27) Olson, D.L. and Matlock, D.K, ASM International,Corrosion of Weldmets (Product code 05182G),1993
- 28) Kadirgan, F. and Suzer, S., Electrochemical and XPS studies of corrosion behavior of low carbon steel in the presence of FT2000 inhibitor, Journal of electron spectroscopy,114-116 (2001) 597-601.
- 29) Cheng, Y.F. and Steward, F.R., Corrosion of carbon steels in high-temperature water studied by electrochemical techniques, Corrosion Science 46(2405-2420), 2004.
- 30) Srinivasan, P.B., Muthupandi, V., Dietzel, W., and Sivan, V., An Assessment of Impact Strength and Corrosion behavior of Shielded Metal Arc welded dissimilar weldments between UNS 31803 and IS 2062 steels,2006, Material and Design 27 ( 182-191).
- 31) Yayla, P., Kaulc, E. and Ural, K., Effects of welding processes on the mechanical properties of HY 80 steel weldments, Materials and Design 28 (2007) 1898–1906.
- 32) Kanjilal, P. and Pal, T.K., Combined effect of flux and welding parameters on chemical composition and mechanical properties of submerged arc weld metal, Journal of Materials Processing Technology 171 (2006) 223–231.
- 33) Babu, S.P K. and Natranjan, S., Corrosion behavior of Pulsed Gas-Tungsten Arc weldments in Power plant C-steel, JMEPEG 16(2007)620-625.
- 34) Babu, K.S.P. and Natranjan, S., Influence of Heat input on high temperature weldment in SAW welded power plant steel,2007, Material and Design 29 (2008) 1036-1042.
- 35) Babu, S.P.K. and Natranjan, S., High temperature corrosion and characterization studies in Flux cored arc welding 2.25Cr-Mo Power plant steel, JMEPEG 19(2010): 743-750.
- 36) Lee, D.J., Jung, K.H. and J.H. Sung, Pitting corrosion behavior on crack property in AISI 304L weld metals with varying Cr/Ni equivalent ratio, Materials and Design 30 (3269–3273),2009.
- 37) N.A. Mcpherson, T.N. Baker, and D.W. Millar, A Study of the Structure of Dissimilar Submerged Arc Welds, journal of metallurgical and materials transactions, Pg 823-833, 1998

- 38) Vera Lucia Othe´ro de Brito, Herman Jacobus Cornelis Voorwald, Nasareno das Neves, and Ivani de S. Bott, Effects of a Postweld Heat Treatment on a Submerged Arc Welded ASTM A537 Pressure Vessel Steel, *Journal of Materials Engineering and Performance*, Pg 249-257, 2001
- 39) Abilio Manuel Pinho De Jesus, Alfredo S. Ribeiro, Antonio A. Fernandes, Influence of the submerged arc welding in the mechanical behaviour of the P355NL1 steel—part II: analysis of the low/high cycle fatigue behaviours, , *Journal of materials science*, Pg 5973-5981, 2007
- 40) Saurav Datta & Goutam Nandi & Asish Bandyopadhyay & Pradip Kumar Pal, Application of PCA-based hybrid Taguchi method for correlated multicriteria optimization of submerged arc weld, *Journal of Advanced Manufacturing Technology*, Pg 276-286, 2009
- 41) H.-S. Moon<sup>1</sup> and R. J. Beattie, Development of Adaptive Fill Control for Multitorch Multipass Submerged Arc Welding, *Journal of Advanced Manufacturing Technology*, Pg 867-872, 2002
- 42) By E. Baune, C. Bonnet and S. Liu, Reconsidering the Basicity of a FCAW Consumable — Part 1: Solidified Slag Composition of a FCAW Consumable as a Basicity Indicator, *journal of Supplement to the welding*, Pg 57-65, 2000
- 43) Saurav Datta & Asish Bandyopadhyay & Pradip Kumar Pal, Solving multi-criteria optimization problem in submerged arc welding consuming a mixture of fresh flux and fused slag, *Journal of Advanced Manufacturing Technology*, Pg 935-945, 2006
- 44) Vinod Kumar Dr. Narendra Mohan Dr. J.S.Khamba, Development Of Cost Effective Agglomerated Fluxes From Waste Flux Dust For Submerged Arc Welding, *Proceeding the world congress of engineering*, 2009

